Resolving the Impacts and Feedback of Ocean Optics on Upper Ocean Ecology

W. Paul Bissett
Florida Environmental Research Institute • Tampa, Florida USA

Oscar Schofield, Scott Glenn
Rutgers University • New Brunswick, New Jersey USA

John J. Cullen, William L. Miller
Dalhousie University • Halifax, Nova Scotia Canada

Albert J. Plueddemann
Woods Hole Oceanographic Institution • Woods Hole, Massachusetts USA

Curtis D. Mobley
Sequoia Scientific, Inc. • Redmond, Washington USA

December 30, 1831 – "The deep water differs as much from that near shore, as an inland lake does from a little pool. – It is not only the darkness of the blue, but the brilliancy of its tint when contrasted with the white curling tip that gives such a novel beauty to the scene."

—Charles Darwin, *The Beagle Diaries*

Introduction

The abundance and fecundity of life on this planet is directly related to the energy supplied by the sun. The pyramid of life starts with the absorption of a fraction of this energy, followed by its conversion from electromagnetic to chemical energy (photosynthesis) and its subsequent storage into biomass (primary production). This chemical energy supports, in one way or another, the myriad of food webs that exist on the earth[1]. Thus, the study of food webs and their dynamics is to a first order defined by the basic energy inputs into the ecosystem, and therefore the study of life requires understanding of the amount of energy available to feed biological systems.

The study of energy propagation to the planet is called geophysical optics, and is sub-divided into two categories, meteorologic optics (energy and atmosphere) and hydrologic optics (energy and water; Preisendorfer, 1976). The majority of solar energy striking the earth falls into two broad bands of the electromagnetic spectrum, visible energy (approximately 400 to 700 nm) and infrared energy (700 nm to 100 µm). As water is nearly opaque to infrared energy (Figure 1), the study of ocean optics has been primarily concerned with propagation of visible energy, i.e. light. This is also a natural starting point for the study of ocean ecology as photosynthesis is driven (with a few exceptions) by energy within the visible light spectrum, which has sufficient energy per photon to induce photochemistry. As phytoplankton accumulations also impact the color and clarity of the water column, there is a direct link between the studies of ocean optics and ocean ecology (Yentsch and Phinney, 1989).

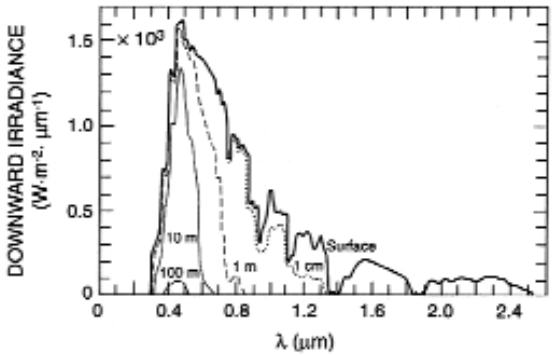

Figure 1. *Spectrum of downwelling irradiance at the sea surface and at various depths within the upper ocean. From Kraus and Businger (1994), "Atmosphere Ocean Interaction". Copyright Oxford University Press.*

[1] We are ignoring chemosynthesis using reduced inorganic molecular products around hydrothermal vents.

Photosynthetic organisms grow and alter the fundamental optical aspects of the medium in which they exist; as phytoplankton grow and accumulate, the total light absorption increases, reducing the total light flux to deeper levels. Thus, the very act of photochemical conversion of visible energy to biomass is a negative biological feedback, creating instabilities for the future growth rate of the phytoplankton (Lorenzen, 1972). This reduction of light is evident to the eye, as areas rich in phytoplankton appear darker, less transparent, and more "green" than in areas where phytoplankton are less abundant. It was this effect to which Charles Darwin was referring in his entry to his diaries. In turn, the quantitative recognition of the influence of phytoplankton absorption on ocean color (Yentsch, 1957; Yentsch, 1960) led to the creation of the Coastal Zone Color Scanner (CZCS) satellite, launched in 1978 (Mitchell, 1994), and more recently the Sea Wide Field of View Sensor (SeaWiFS), launched in 1997 (Figure 2). These sensors firmly established the relevance of ocean optics to a broad suite of physical, chemical, and biological oceanographic studies.

Circulation and water column mixing are constantly moving the phytoplankton relative to a particular light level and to each other. Diurnal, seasonal, and latitudinal variations in visible and infrared energy supply drive differential heating and cooling of the ocean and atmosphere. The differences of energy delivery combined with other geophysical processes, e.g. latitudinal variations in the vertical component of the earth's rotation, drive a coupled ocean-atmospheric system that yields winds, waves, and currents. On a global scale, the sum of these physical interactions on the ocean results in a thermo-haline circulation pattern (Broecker and Takahashi, 1985). This circulation pattern helps determine the global distribution of chemical, biological, and optical material in the ocean. On a local scale, atmospheric-oceanic interactions yield winds, waves, and precipitation that determine the vertical mixing of the water column. Such mixing controls the location of phytoplankton with respect to the incoming visible energy, as well as the supply of nutrients from areas of lower concentrations to areas of higher concentrations (Figures 3 and 4). Thus, the distribution of phytoplankton will depend on the physical movement of water, as well as the propagation of light through the water column.

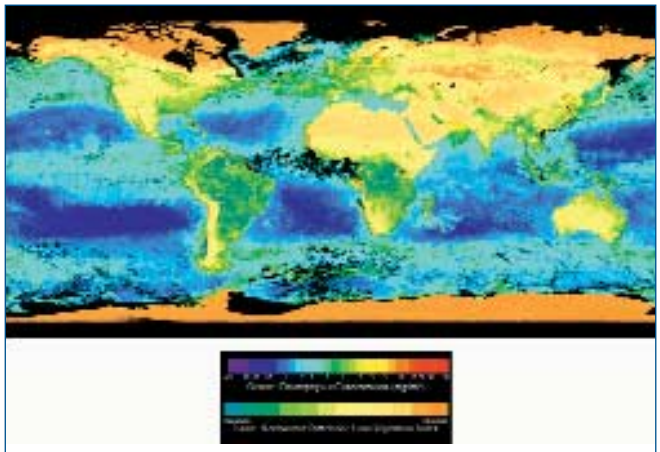

Figure 2. *Global SeaWiFS Composite image for March 2000 (provided by the SeaWiFS Project, NASA/Goddard Space Flight Center and ORBIMAGE). Ocean blue indicates areas of low phytoplankton pigments; red indicates areas of high phytoplankton pigments. The color bar at the bottom displays the pigment concentrations associated with each color. On a global scale the warm oligotrophic gyres contain lower pigment concentrations than the colder, high latitude and the coastal regions. This is a function of higher solar irradiance, lower wind-driven mixing, and higher stratification in oligotrophic regions that result in a nutrient-poor euphotic zone. This figure displays the general inverse relationship between sea surface temperature and phytoplankton biomass.*

Water column chemistry plays a critical role in the growth and accumulation of phytoplankton. To consider its importance in a broad sense, one might divide chemical processes into two components: those that require direct chemical absorption of sunlight (photochemistry) and those that do not. The cycling and supply of inorganic and organic elements necessary for phytoplankton growth can depend on both types of reactions. For the most part, the cycling of inorganic macro-nutrients such as nitrogen, phosphorous and silica do not depend on photochemistry. The dissolved concentrations of these nutrients in the photic zone are most often related to biological activity in the water with plant growth removal and microbial regeneration. Physical mixing from locations of high concentration to low concentration is also important and can completely overshadow in situ chemical processes in some areas. The supply of other essential micro-nutrients such as cobalt, iron, manganese, and vitamins can rely on biological, "dark" chemical, as well as photochemical reactions.

Photochemistry depends on the direct absorption of sunlight, predominantly by complex organic molecules and less often by inorganic compounds. Direct effects of this light absorption (mainly from high energy ultraviolet [UV] radiation with wavelengths less than 400 nm) include photo-destruction of chemical bonds and fragmentation of the complex molecule into smaller, different compounds. Secondary reactions between energized organic molecules and dissolved oxygen in seawater will also form highly reactive compounds such as hydrogen peroxide and hydroxyl radicals. The overall result of these photochemical reactions can both promote (by breaking down complex molecules and increasing accessibility of organic carbon and some inorganic nutrients) and retard (by damaging cellular constituents) biological processes.

The supply of organic chemicals by biological and

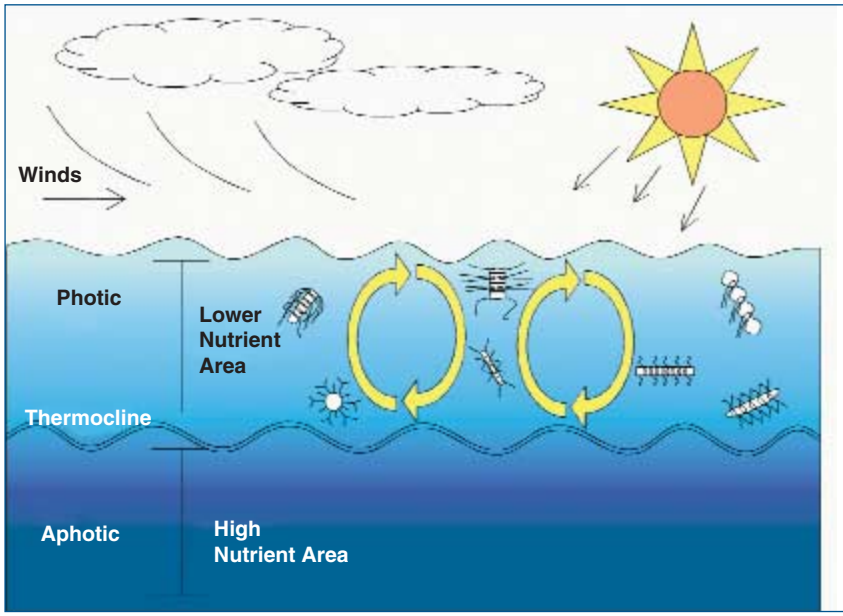

Figure 3. *In cooler, high-wind environments, water is mixed down to the base of the seasonal thermocline, increasing the supply of nutrients to the sun-lit waters and supporting higher levels of phytoplankton biomass, larger phytoplankton species, and lower water clarity.*

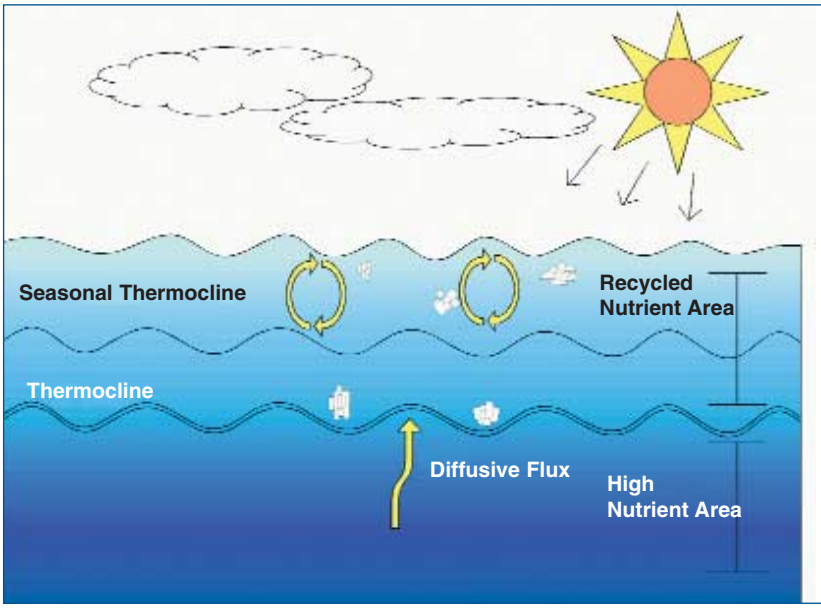

Figure 4. *In warmer, lower wind environments, water is only shallowly mixed, and surface phytoplankton quickly exhaust ambient nutrient supplies. Total phytoplankton populations are small, dominated by smaller species. Those trapped in the surface mixed layer are supported mainly by regenerated production, while those at the deepest levels are supported by small diffusive supplies across the main thermocline.*

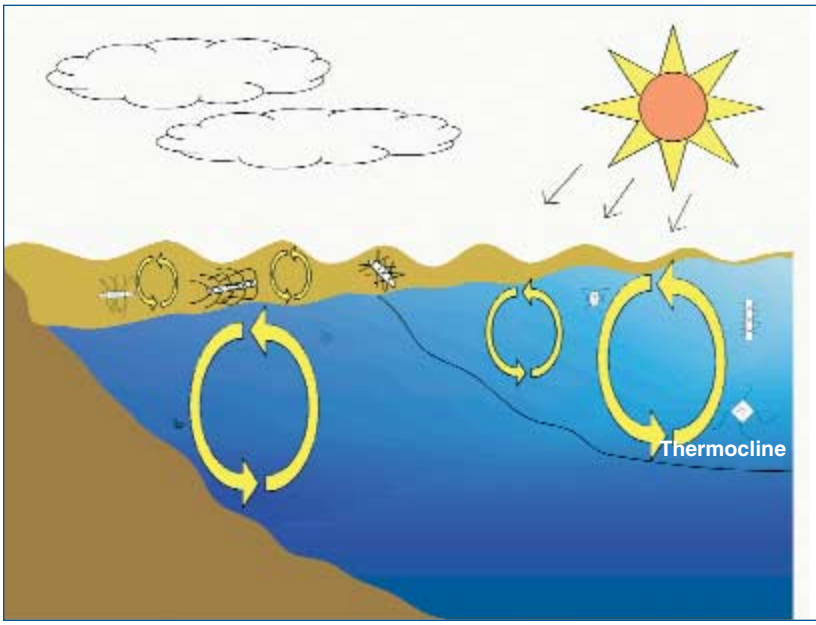

Figure 5. *River discharge supplies both nutrients for phytoplankton growth, and dissolved matter that reduces water column clarity. The river water is less dense, than the ambient ocean water, so that the buoyant plume riding atop the denser ocean water acts to stratify the near-surface water column until it is dispersed via mixing and dilution processes. Near shore, the more highly attenuating plume decreases light intensity below the plume, reducing phytoplankton growth within the underlying ocean water. As the river plume spreads and mixes down, the clarity of the water column increases, allowing light and nutrients to penetrate to deeper depth.*

physical processes changes ocean optics, particularly in the coastal environment where terrestrial runoff and river outflows may provide dark, organic rich waters to nutrient-limited ocean regimes (Figure 5). These buoyant outflows not only concentrates photochemical activity near the surface, but also attenuates biologically and photo-chemically active UV, protecting biological components from damage (Arrigo and Brown, 1996). The example in Figure 5 of water column optical constituents illustrates the physical, chemical, and biological processes that drive the distribution of inherent optical properties in the ocean. Thus, the study of ocean optics requires a clear understanding of the oceanic ecological system. By extension, it is also clear that the study of upper water ocean ecology requires a clear understanding of ocean optics. These two fields are intricately linked and one could argue that future developments in either of these fields will require integrated approaches to both of their studies.

While the early development of the individual fields of physical, biological, chemical, and optical oceanography tended to be separate lines of inquiry, early scientists concerned with oceanic ecological processes, such as Henry Bigelow, realized that knowledge in this field will only result from inter-disciplinary approaches. These problems are some of the most difficult in oceanography. Modern day oceanographers are asked ecology-based questions similar to those posed to the Kiel Commission in 1870, recognized as the first organization focused on an oceanographic problem—the prediction of Prussian fisheries yields (Mills, 1989). In particular, oceanographers are asked to determine the controlling mechanisms for the distribution of plants and animals in the ocean, and are increasingly asked to forecast the impacts of short-term weather, long-term climatic, and anthropogenic changes to these distributions. Forecasting requires understanding the individual physical, chemical, biological, and optical response functions to a forcing event, as well as the feedback of those responses into the larger combined system. In theory, quantification of energetic responses and system feedbacks could yield a prognostic framework within which to study, and hopefully predict, upper ocean ecology. This quantification would also yield a method to predict the optical properties of the water column. While oceanographers have made great strides in forecasting abilities since that first commission, there is still a great amount of work to be accomplished. Thus, this paper will discuss the impact of solar irradiance on the individual physical, chemical, and biological components of oceanography, and discuss methods for resolving these impacts and their feedbacks into a predictive ecological model.

Optics and Physical Processes

Ocean optics and physical processes are fundamentally linked via the radiative heating component of solar radiation absorbed by the ocean water mixture (pure water + particulate and dissolved matter). Of particular interest is the influence of radiative heating on sea surface temperature (SST) and near-surface stratification (the rate of change of density with depth). Since solar radiation penetrating the atmosphere has a spectral distribution, i.e. each wavelength contains a varying fraction of the total downwelling energy, the distribution of radiative heating in the water column is dependent on both the spectra of incoming light and spectrum of optical properties of the water column.

Penetrative Radiation and Upper Ocean Heating

The solar radiation that reaches the sea surface is concentrated in the visible and near infrared. Of the energy that penetrates the ocean surface, the vast majority (> 99%) of infrared is absorbed within the first 1.5 m of the water column (Figure 1), but within the visible part of the spectrum, the depth of penetration varies dramatically with the optical characteristics of the water (Figure 6). The radiation absorbed in the upper ocean is converted to heat and its depth-distribution is determined by the transmission function, $T(\lambda,z)$. Although $E_d(0^-)$, the surface downwelling irradiance just above the sea surface (see Box 1 for definitions of optical properties), is routinely obtained locally from ships and buoys during oceanographic experiments, and can be obtained globally from satellite remote sensing products, T is not routinely measured. Instead, various parameterizations are used to account for the expected depth dependence of T for discrete wavelength bands. For most water types, variability in T is

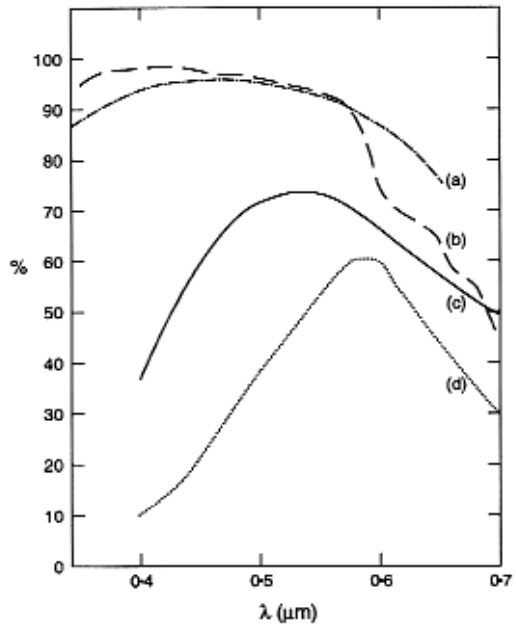

Figure 6. The percent transmittance in the visible band through one meter of water for various water types: ***(a)*** *Clear Mediterranean,* ***(b)*** *Crater Lake,* ***(c)*** *coastal: medium transparency,* ***(d)*** *coastal: low transparency (Kraus and Businger, 1994). Copyright Oxford University Press.*

primarily due to phytoplankton pigments, the most ubiquitous of which is chlorophyll a, and this chlorophyll concentration can be used as the basis for a T parameterization. Detailed parameterizations may include more than 100 wavelength bands (Morel and Antoine, 1994), while more commonly used parameterizations (e.g. Paulson and Simpson, 1977) use just two bands. It has been shown that a high degree of fidelity in reproducing the vertical structure of T below the first 10-30 cm can be obtained by using between three and four bands in models of penetrating radiation and local heating (Kantha and Clayson, 1994; Morel and Antoine, 1994; Ohlmann and Siegel, 2000).

The impact of the absorbed radiation on the SST is a complicated inter-play between the net surface heat flux T, the rate of mixing just below the sea surface, and the depth to which this mixing occurs. This depth is typically called the Mixed Layer Depth (MLD). When surface irradiance is large and mixing rates are low (e.g. on calm, clear days in the tropics), the effect of radiative heating can be dramatic (Figure 7). Seasonal changes in SST and stratification, although on significantly different time and depth scales, are strikingly similar in character to diurnal changes (Figure 8). In both cases it is notable that relatively well-mixed, nutrient rich water is "temporarily" (e.g. for a day or a season) isolated from the surface by strong, near surface thermal stratification. Thermal stratification is gradually introduced to deeper water by the blue-green portion of the irradiance spectrum. The deeper water remains isolated until surface heat losses and/or increased mechanical mixing are sufficient to break

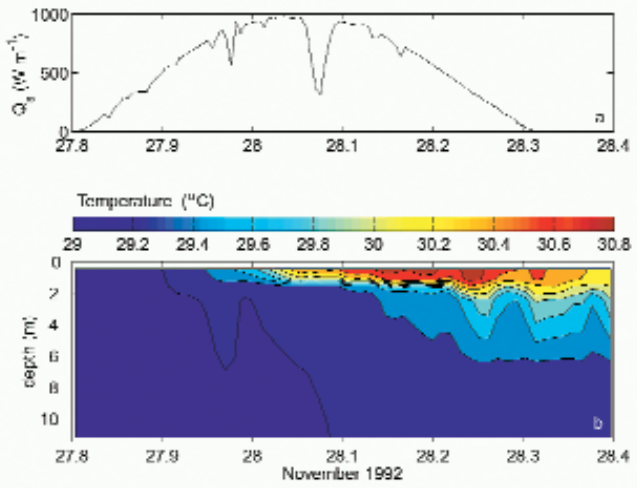

Figure 7. *Radiative heating of the upper ocean under low wind conditions.* ***(top)*** *Shortwave (285-2800 nm) downwelling irradiance at the sea surface and* ***(bottom)*** *Temperature vs. depth and time for a site in the western tropical Pacific (1.75°S, 156°E). The pre-dawn MLD was about 30 m. Wind speed during the day was ≤ 2 m/s. The strongest heating was within the upper 1.5 m due to the absorption of infrared radiation, and SST increased by nearly 2° C.*

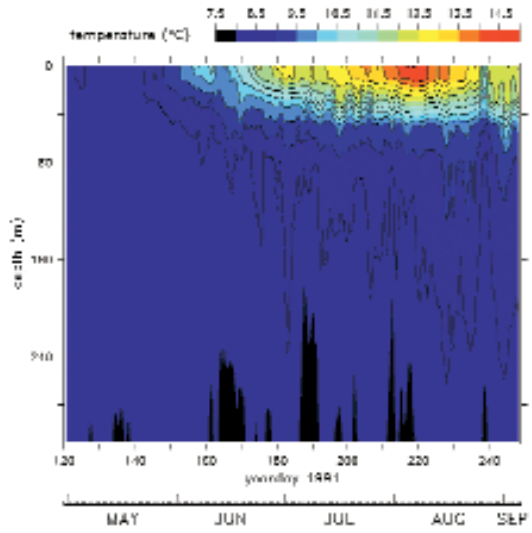

Figure 8. *Contours of daily average temperature from a site in the subarctic north Atlantic (59.5°N, 21°W). The "spring transition" from net surface cooling and nearly uniform upper ocean temperature to net heating and the establishment of near-surface stratification is seen near 22 May. The rate of change of upper ocean heat content was approximately balanced by the surface heat flux from mid May through early August (Plueddemann et al., 1995). Copyright American Geophysical Union.*

down the near-surface stratification. On daily time scales, the absence of downwelling irradiance at night is the principal factor, whereas on seasonal time scales the gradual reduction of daily average downwelling irradiance, the increase in atmospheric storm activity, and the presence of oceanic fronts and eddies all play a role. The breakdown of stratification brings nutrients and stored heat back in contact with the surface.

Because the ocean's immediate impact on the atmosphere is largely determined by SST, which modulates the transfer of sensible and latent heat, the cycle of heat storage and release in the upper ocean are crucial to regulating the rate at which the ocean responds to atmospheric forcing and how it feeds back to the atmosphere. Some heat is sequestered below the MLD on seasonal time scales throughout the worlds' oceans, but in the tropics, where the downwelling surface irradiance is large, the water is clear, and the MLD is shallow, this process can be important on inter-annual and longer time scales (Figure 9). The fact that the heat flux to depths below the annual maximum MLD can be a significant fraction of the annual mean for much of the tropics (Lewis et al., 1990) indicates that that coupled air-sea models that seek to predict weather patterns and ocean currents require accurate parameterizations of spectral transmission within these regions.

The Diurnal Cycle of Thermal Stratification

While daylight reliably produces net surface heat-

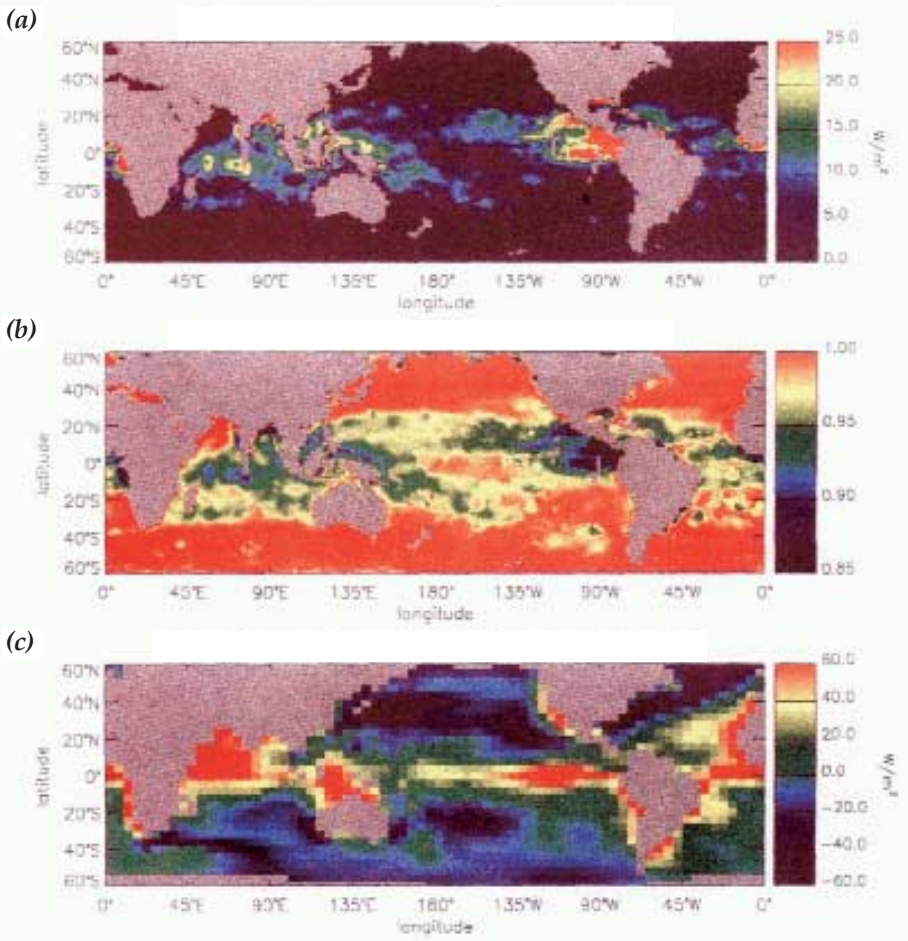

Figure 9. ***(a)*** *Estimates of the net irradiance at a depth equal to the largest climatological monthly-mean MLD. This represents the heat flux into water that is below the annual maximum MLD.* ***(b)*** *The fraction of net irradiance just below the sea surface that is converted to heat within the mixed layer on an annual basis. At high latitudes all of the surface heat flux goes into mixed layer heating. In the tropics, as much as 15% of the surface heat flux goes towards heating waters deeper than the annual maximum MLD.* ***(c)*** *Climatological mean air-sea heat flux. Comparison with (a) shows that the heat "lost" from the mixed layer due to penetrative radiation can be a significant fraction of the total heat flux in some locations (Ohlmann et al., 1996). Copyright American Meteorological Society.*

ing, radiative cooling (quasi-black body longwave emission) along with sensible and latent heat losses typically produce net surface cooling at night. Strong diurnal cycling of MLD can result when daytime heating and nighttime cooling are of similar amplitude (Figure 10). If not properly accounted for, this variability in stratification can confound attempts to determine the mean vertical structure of any physical, chemical, or biological property that is strongly affected by stratification. Attempts to determine the vertical structure of the wind-driven velocity illustrate this problem.

Because mass and momentum are mixed vertically in a similar way, there is a diurnal cycle in the penetration depth of the wind-driven velocity that corresponds to the MLD. Price et al. (1986) showed that during periods of diurnal cycling in MLD the time-average velocity had a vertical structure that is similar to an Ekman spiral. However, the classical Ekman spiral is derived in the absence of vertical stratification, whereas the spiral described by Price et al. (1986) is primarily due to the temporal variability of stratification. With sufficient vertical resolution, the underlying structure of velocity, i.e. without the "smearing" due to MLD cycling, can be determined by time averaging in a vertical coordinate relative to the (changing) stratification rather than at fixed depth. Plueddemann and Weller (1999)

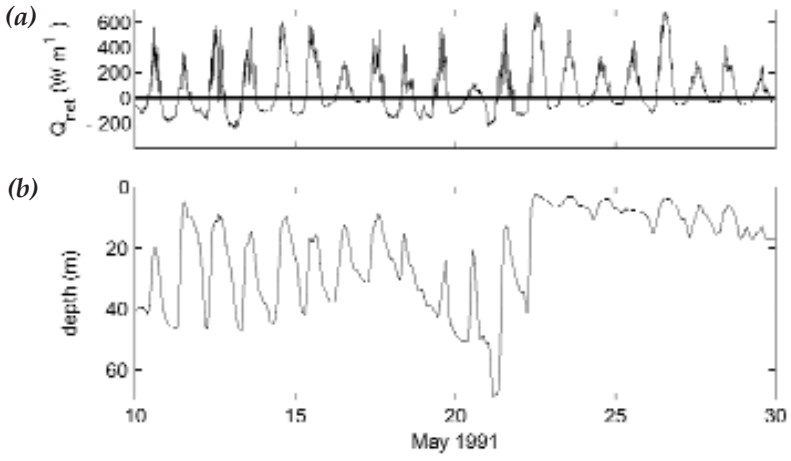

Figure 10. *Time series of* ***(a)*** *net heat flux and* ***(b)*** *MLD for a site in the subarctic north Atlantic (59.5°N, 21°W). Note the strong diurnal cycling of MLD during the first 10 days in response to relatively strong nighttime cooling and weak daytime heating. MLD variability is reduced abruptly when the nighttime cooling is decreased.*

found that time-averaged velocity profiles in a coordinate system tied to MLD showed a tendency for "slab-like" flow in the mixed layer with shear and rotation concentrated in a weakly stratified transition layer below it.

This result is consistent with a high-viscosity mixed layer where particles are mixed rapidly, and a transition layer characterized by lower viscosity, partial mixing, and shear instability. It is likely that the distinct properties of these two layers influence bio-optical variability through particle re-distribution and nutrient dynamics. In order to investigate such influences in observations and models, it is necessary to determine the diurnal cycle of heating and cooling (which requires knowledge of the air-sea heat flux and an accurate representation of T) and to resolve the variability in MLD (which requires high vertical resolution).

Feedbacks

The transmission function can vary significantly on synoptic time scales as a result of changes in particle type and concentration. The principal effect results from the change in the distribution of phytoplankton. Consistent with estimates based on satellite observations and climatological surface heat fluxes and density profiles (Lewis et al., 1990), study in the tropical Pacific, where irradiance and chlorophyll profiles were measured simultaneously, found an increase in the radiant heating rate of 0.11° C per month in the upper 30 m associated with a phytoplankton bloom that followed a westerly wind event (Siegel et al., 1995). A feedback mechanism was suggested whereby wind events deepen the generally shallow MLD, bringing up nutrients from below and setting off a phytoplankton bloom. The increase in phytoplankton concentration increases SST via enhancement of near-surface heating rates. The increased SST may then increase vertical convection in the atmosphere and hasten the decay of the westerly wind event.

Variability in the concentration of phytoplankton may also play a role in regulating SST on seasonal time scales. In particular, there is the possibility of positive feedback between near-surface stratification and biological production (Sathyendranath et al., 1991). In this scenario, increased thermal stratification resulting from increased phytoplankton concentration results in a shallow MLD and reduces the likelihood that synoptic surface forcing will significantly deepen the MLD. Reduction of the depth of mixing may help to keep phytoplankton within the sunlit surfaces waters, where the rate of phytoplankton production exceeds the rate of phytoplankton respiration. If there are sufficient nutrients, the "trapping" in the upper photic zone by the shallow MLD provides more favorable conditions for growth. Increased growth yields a greater production of biomass and pigments that reduces the transmission of radiant energy, which increases stratification and reinforces the bloom response. Nonuniform distributions of phytoplankton in stratified waters can also interact with penetrating solar irradiance to influence thermal structure. In tropical waters, the typical increase of chlorophyll concentration (hence absorption of light by phytoplankton and concomitant local heating) can give rise to local heating rates that increase with depth (Lewis, 1987). This can lead to vertical motions influenced directly by biological processes.

The increasing interest in climatological variability in the world's oceans has stimulated interest in the role of penetrative radiation in regulating SST variability and air-sea interaction on long time scales. A complete assessment of potential feedbacks would require a coupled global ecosystem model with near-surface vertical resolution of order 1 m. These requirements are beyond present capabilities. However, the impact of penetrative radiation can be assessed by including progressively more realistic parameterizations of T. In a recent study, Murtugudde et al. (in press) considered the impact of including a spatially variable T (based on satellite ocean color data) in an Ocean General Circulation Model (OGCM), rather than a constant penetration depth. They concluded that some of the limitations of commonly used (constant penetration depth) OGCMs, such as under-estimation of SST in the eastern tropical Pacific cold tongue, may be due to inaccurate representation of T (Figure 11). Progress in the prediction of atmospheric and oceanic systems will require explicitly addressing the temporal and spatial variability of ocean optical properties, and their impacts on the air-sea heat flux.

Optics and Chemical Processes

The close link between optical and chemical processes in the ocean is a relatively new development. The link has largely strengthened as the field of marine photochemistry has evolved over the last 20 years from a novelty to a necessity in the study of elemental cycling, ocean optics, and ecological models of the upper ocean. Over the past two decades, we have discovered that the majority of ultraviolet sunlight (<400 nm) in the sea is absorbed by chromophoric (colored) dissolved organic matter (CDOM), and that this absorbed energy drives photochemical reactions in the surface ocean. The main result of this absorption is to energize electrons within the CDOM: an event that leads to the breaking of molecular bonds and the production of a suite of chemically distinct organic compounds. It also initiates secondary reactions between "excited" CDOM and other chemicals in the surrounding seawater, mainly oxygen, to drive the oxidation and reduction of chemical compounds such as trace metals and sulfur compounds. As these photochemical reactions proceed, the surface water optical properties change, with a concomitant accumulation of photochemical reaction products that include a complex mixture of reactive oxygen species, inorganic nutrients, and

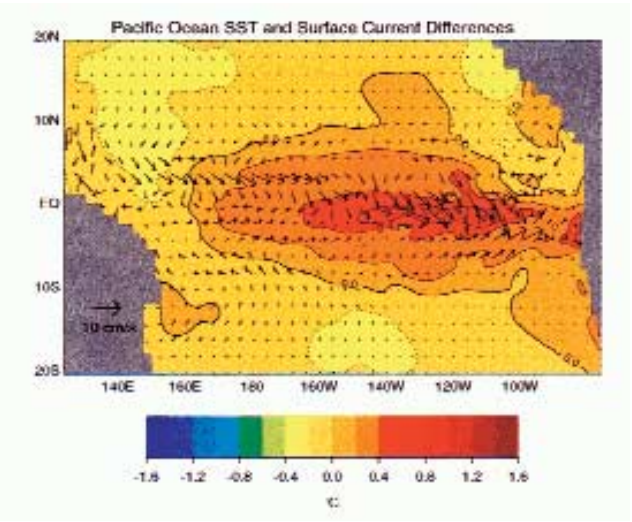

Figure 11. *Annual mean difference in SST (contours) and surface currents (arrows) for an OGCM with spatially variable attenuation depth relative to one with a constant attenuation depth of 17 m. In both cases the depth dependence of penetrative radiation is parameterized using a single exponential function (Murtugudde et al., 2001). Copyright American Meteorological Society.*

trace gases. These reaction products may also cause changes in the biological availability of dissolved organic matter.

The Photochemical Driver: CDOM

The absorption of solar radiation by CDOM is the pivotal event that drives most aquatic photochemistry and its subsequent involvement in biogeochemical process in natural waters. The CDOM present in seawater is a complex mixture of biochemical breakdown products originating in terrestrial, freshwater, and marine systems. Interestingly, while phytoplankton production undoubtedly supplies the majority of the biochemical starting materials in the open ocean that comprise "marine" CDOM, a tight coupling between phytoplankton and CDOM concentration is not always observed (Rochell-Newall et al., 1999; Del Castillo et al., 2000). The literature supports terrestrial runoff (Nelson and Guarda, 1995; Nieke et al., 1997), coastal sediments (Rochell-Newall et al., 1999; Boss et al., 2001), and *in situ* microbial processes (Nelson et al., 1998; Rochell-Newall et al., 1999; Del Castillo and Coble, 2000; Letelier et al., 2000) as the dominant sources for CDOM in the ocean. Of course, the relative importance of these sources depends greatly on location and local hydrographic conditions, and seasonal cycles of CDOM are observed in both coastal (DeGrandpre et al., 1996; Kuwahara et al., 2000; Kahru and Mitchell, 2001) and open ocean settings (Nelson et al., 1998).

While some progress has been made, a precise picture of the complex suite of chromophores that CDOM represents has not yet been presented. Virtually all natural waters confirm this complexity of potential electron transitions and chemical functionality, and this complexity can be seen in the smooth exponential decrease in CDOM absorbance from the UV to the visible portion of the spectrum. CDOM UV absorbance dominants UV absorption in the ocean and even in the clearest open ocean waters makes up as much as 50% of the non-water "blue" absorbance (440 nm; Nelson et al., 1998). As a consequence of this spectral absorption shape, the energetic UV radiation in sunlight is the principal component that drives photochemistry in the ocean.

While CDOM is thought to have several sources in the ocean, a single process is believed to dominate its sink. As CDOM initiated photochemistry proceeds, there is a loss of the ability to absorb radiation across the entire CDOM absorbance spectrum due to chromophore degradation. This process is called photobleaching or photochemical fading and is observed both in laboratory irradiations (Gao and Zepp, 1998; Grzybowski, 2000) and in the field (Siegel and Michaels, 1996; Vodacek et al., 1997; Nelson et al., 1998). Fading alters both the spectral driver for photochemical reactions and the inherent optical properties of natural surface waters.

To examine the rate of fading at a given wavelength, one must quantify the amount of radiation absorbed by CDOM and the efficiency with which CDOM loses its color (i.e. how much absorbance is lost per photon absorbed?). To complicate these seemingly simple relationships, CDOM both absorbs radiation and photo-bleaches poly-chromatically. In other words, for every single wavelength of light absorbed by CDOM, color loss occurs not only at the absorbed wavelength, but also across the entire absorbance spectrum. For this reason, the photochemical efficiency of CDOM fading cannot be described with a simple two-dimensional function (product vs. wavelength) like many other photochemical reactions. New three-dimensional approaches that define photochemical fading with efficiency surfaces, such as the one shown in Figure 12, are being developed to quantitatively describe the spectral response for CDOM fading and integrate this process into ecological models that include photochemical product formation and changing biological damage from UV radiation. The impact of this second effect is discussed below.

Photochemical Products

Some 25 years ago, Zafiriou (1977) published a "preview" of the field of marine photochemistry that contained predictions of its potential significance in marine chemistry. From that point on, a great number of papers have tested those predictions and uncovered a wide variety of additional photochemical processes in both fresh and saltwater environments. A cursory survey of the sunlight-induced processes (other than fad-

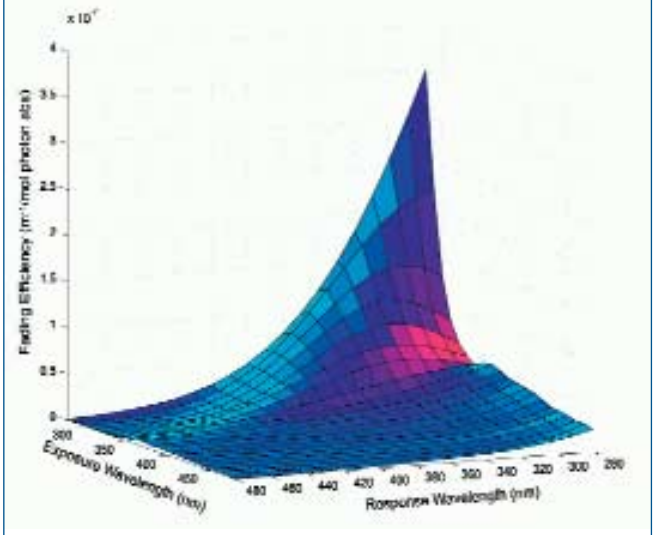

Figure 12. *A 3-dimensional surface describing the photochemical fading efficiency of chromophoric dissolved organic matter (CDOM) in the surface ocean. The efficiency of this process (the height of the surface in the figure) is defined as the change in CDOM's capacity to absorb radiation at a particular wavelength per photon of radiation absorbed at any given wavelength. The "exposure wavelength" axis represents the radiation absorbed by CDOM which causes fading and the "response wavelength" axis represents the position in the CDOM spectrum that fading occurs. Note that fading is most efficient when high-energy UV-B radiation (< 320 nm) is absorbed by CDOM and that fading at wavelengths below 350 nm is more efficient than longer wavelengths regardless of the wavelength absorbed.*

ing) that constitute feedbacks to ocean ecology includes trace gas reactions, trace metal and radical chemistry, and the fragmentation and alteration of dissolved organic carbon (DOC).

Several atmospherically reactive trace gases such as carbonyl sulfide (OCS; Andreae and Ferek, 1992; Weiss et al., 1995; Uher and Andrea, 1997; Preiswerk and Najjar, 2000), carbon disulfide (CS_2; Xie et al., 1998), methyl iodide (CH_3I; Moore and Zafiriou, 1994) and carbon monoxide (CO; Valentine and Zepp, 1993) have oceanic sources of global significance that depend on CDOM distributions and photochemical reactions. Dimethyl sulfide (a cloud forming aerosol particle produced by phytoplankton) has a photochemical sink in the ocean. A suite of oxygen radicals (hydrogen peroxide, superoxide, hydroxyl radicals) and reduced metals (iron, copper, and manganese) are also produced by marine photochemistry and can influence surface water redox conditions and subsequent chemical cycles and the biological availability of trace nutrients (reviews by Miller, 1994; Blough, 1995). As CDOM (a subset of the total DOC) undergoes photochemical reactions, there is a general reduction in the average molecular weight of DOC coincident with the production of a large array of low molecular weight (LMW) carbon compounds including carbonyls and organic acids (Miller, 1994; Zepp et al., 1995). Moran and Zepp (1997) recently reviewed the literature on biologically available organic compounds generated by photochemical reactions involving CDOM and listed 13 different carbon substrates from eight separate references.

In 1991, Mopper et al. (1991) reported that carbon monoxide was by far the most rapidly produced carbon photoproduct measurable in seawater at the time. Miller and Zepp (1995) reported that dissolved inorganic carbon (DIC, measured as the sum of carbon dioxide, bicarbonate and carbonate ions) was produced from CDOM about twenty times as fast as carbon monoxide in the near coastal water of the Mississippi River plume. Further comparison by Miller and Moran (1997) found DIC production to be fifteen times as fast as carbon monoxide production for coastal marsh water. Other studies support the fact that the direct

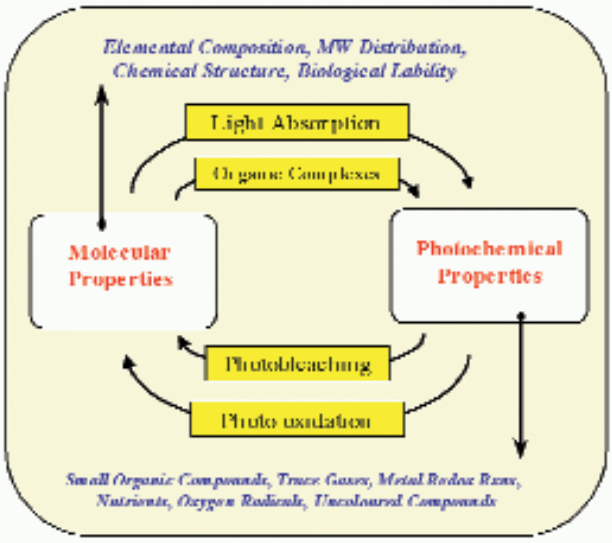

Figure 13. *A simple diagram of the interrelationship between molecular properties of absorbing molecules in the ocean and their photochemical properties. It is a compound's molecular properties (examples in text at top of figure) that determine its potential for photochemical reactivity. (What organic complexes are present? How does it absorb light?) Depending on these molecular properties, photochemistry will result in specific product formation and transformations (examples in text at bottom of figure) and, through photo-oxidation and photobleaching, change the starting molecular properties responsible for photochemical reactivity in the first place. The system is constantly modified by input of new compounds from physical mixing and biological activity and by feedback between photochemical reactions and molecular properties as CDOM and other photoreactive compounds are cycled through the photic zone.*

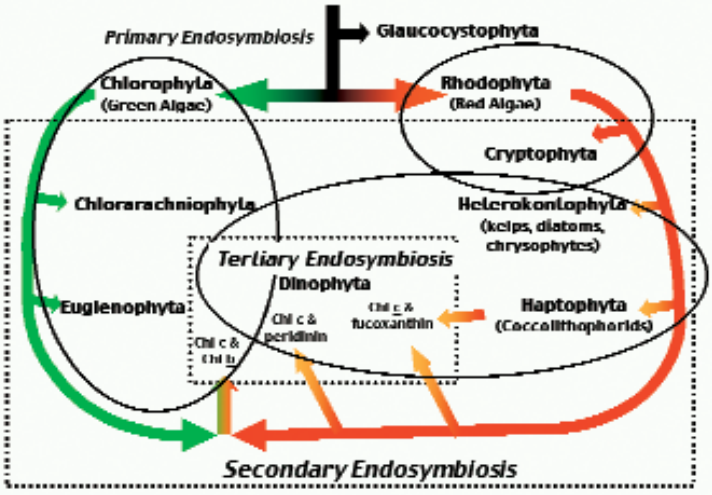

Figure 14. *The proposed evolution of the major classes phytoplankton taxa. Evolution proceeded through a series of endosymbiotic events that are denoted by the squares (dotted lines). The three major spectrally-distinct classes of algae are delineated by circles and current research efforts are focused on developing effective discrimination procedures using remote sensing techniques. Algae fall within the spectrally distinct groups depending on which accessory pigments they contain (chlorophyll c-, chlorophyll b-, and phycobilin-containing plastids). This figure was redrawn and adapted from Delwiche, 1999.*

photo-oxidation of DOC to DIC in natural waters represents the major identifiable photochemical carbon transformation in the ocean (Kuhnle et al., 1972; Chen et al., 1978; Kotzias et al., 1986; Salonen and Vähätalo, 1994; Graneli et al., 1996; Li et al., 1996; Vähätalo et al., 2000) and suggests a significant oxidation pathway for DOC that bypasses the microbial loop and acts as an independent sink for DOC. The photo-production of DIC appears to be the largest non-biological loss process for DOC in the ocean.

The photochemical oxidation of DOC is currently gaining acceptance as an important process for carbon cycling in the ocean. A recent review of this subject by Mopper and Kieber (2000) affirms that photochemical oxidation and/or degradation of DOC, coupled with the consequent changes these processes have on biological carbon assimilation (discussed below), can strongly impact the geochemical cycling of organic carbon in the ocean. Although there is a vast array of consequences of photochemical reactions in the ocean (trace metal reduction, oxygen radical production, nutrient generation, reactive trace gas production and photolysis), most do not quantitatively impact the cycling of DOC and DIC except, perhaps, through their impact on biological processes. The singular exception to this generality is the direct "photo-mineralization" of DOC to carbon monoxide and DIC.

Biological Feedbacks

Since much of the DOC pool in natural waters is not available to the microbial community over time scales from hours to weeks (Moran and Hodson, 1994), the recognition that the photochemical breakdown of CDOM releases biological substrates has fueled research on the significance of photochemistry to secondary biological production in both marine and freshwater systems. Additionally, it is also possible that the photochemical oxidation of CDOM represents a fundamental change in the refractory nature of the larger carbon molecules that cannot be measured as "identifiable" carbon products. In fact, this second process may provide a larger source of consumable DOC than the sum of all the identified products listed in the review of Moran and Zepp (1997) taken together. Miller and Moran (1997) used a mass balance approach to examine this possibility and found the "unidentified" portion of irradiated CDOM accounted for a much greater proportion of carbon used to fuel microbial growth than could be explained by identifiable low molecular weight compounds.

Moran and Zepp (1997) listed six out of eight studies that noted growth enhancement of heterotrophic bacteria in natural samples previously exposed to sunlight. Further work in this area has produced mixed results with some reports of enhanced bacterial production resulting from prior irradiation and others reporting a decrease in production. From these contrasting reports, it appears that, irradiation of terrestrial CDOM and marine CDOM formed *in situ* at depth enhances bacterial production, while irradiation of surface seawater decreases microbial growth (Benner and Biddanda, 1998; Obernosterer et al., 1999; Moran et al., 2000). Obernosterer et al. (2001) have concluded that there is a general inverse relationship between photochemical effects and bioavailability of DOC. In other words, when DOC is already bio-available, photochemistry will decrease its availability to heterotrophic bacteria. On the other hand, DOC that is mainly refractory will be made more available by photochemistry and result in enhanced bacterial growth. Clearly, the feedbacks and relationships between upper ocean ecology and marine photochemical reactions (outlined in Figure 13) are complex, interactive, and require further investigation to establish their significance in ocean ecology.

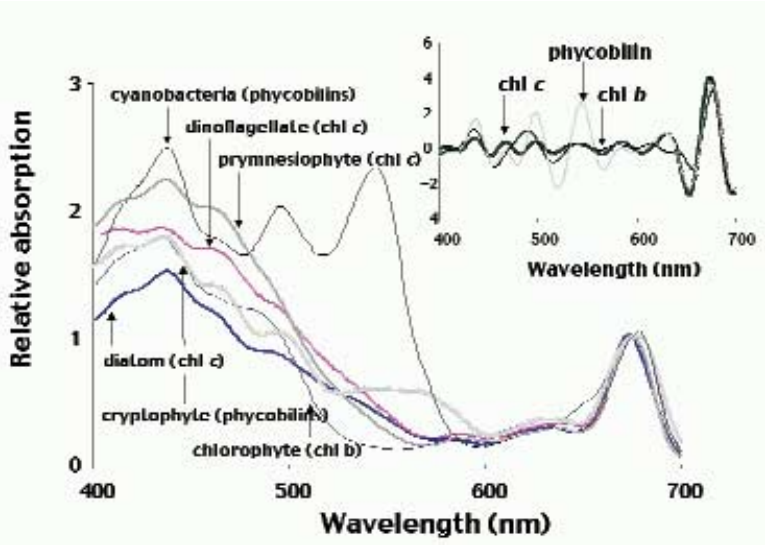

Figure 15. *The wavelength-dependency in the relative (normalized at 675 nm) absorption for the major phytoplankton taxa. The phytoplankton were grown in the laboratory and were low-light acclimated (75 mmol photons m^{-2} s^{-1}) (Johnsen et al., 1994; Schofield et al., 1996). Variabilities in the spectral shapes reflect the presence of different accessory chlorophyll and carotenoid pigments between the phytoplankton groups. The inset illustrates the 4th-dervative spectra for the major spectral classes of algae. The 4th-derivative spectrum is used by chromatographers and phycologists to maximize the minor inflections in absorption spectra (Butler and Hopkins, 1970) in order to resolve the positions of absorption maxima attributable to specific photosynthetic pigments (Bidigare et al., 1989; Smith and Alberte, 1994; Millie et al., 1995).*

Optics and Biological Processes

The biological innovation of photosynthesis, allowing the conversion of radiant energy into chemical energy, represented an epic event in Earth's history. Photosynthesis, which originated more than 3.4 billion years ago (Ba) (Schopf, 1993), had by 2.1 Ba oxidized Earth's atmosphere and surface oceans. Prokaryotic cyanobacteria appeared at least 2.7 Ba (Brocks et al., 1999) and were central to these global changes. By 1.2 to 1.0 Ba the eukaryotic algae arose and diverged into the "green" and the "red" algal lines. These "green" and "red" lines ultimately gave rise to the chlorophytic and chromophytic algae respectively (Figure 14).

The evolution and diversification of the phytoplankton plastids into the three major spectral algal classes resulted from a series of primary, secondary and tertiary endosymbiotic events from the phagotrophic engulfment of photoautotrophs by eukaryotic heterotrophs (Figure 12; Delwiche, 1999). These classes represent three spectrally distinct groups of phytoplankton containing different suites of pigments (Chl c-containing, Chl b-containing, phycobilin-containing; Figure 15). In phytoplankton cells, the pigments are organized with proteins into light harvesting complexes (LHCs) and are used to harvest visible energy to fuel the photosynthesis (Figure 16). These LHCs differ in both the structure and function between the different classes of phytoplankton (Falkowski and Raven, 1997). As these three classes are spectrally distinct (Figures 15 and 17), they can potentially be differentiated optically (Schofield et al., 1999), and by virtue of their abundance represent a major source of color in the ocean.

Phytoplankton regulate the size and composition of the LHCs in response to changes in the incident light field. This results in changes in chemical composition and photosynthetic responses to light (Falkowski and LaRoche, 1991). As the phytoplankton themselves are major sources of energy attenuation, the feedbacks between growth and optimization are cause for constant adjustment. The process of photosynthetic acclimation involves increasing the optical cross-section of the LHCs under low light conditions and decreasing the LHC cross-section under high light. The absorbed light initiates a chain of cascading reactions extending to oxygen evolution, carbon fixation, and growth (Figure 16), and the regulation of pigment synthesis, as well as the allocation of other products of photosynthesis, is directed toward a rough balance between the absorption of light and its utilization in photosynthesis. The balance between absorption and utilization can be represented as "excitation pressure" (Maxwell et al., 1994, 1995). It is directly related to the reduction state of the plastoquinone pool (Figure 17) and it can be approximated in models as the ratio of absorbed to utilized radiation (Geider et al., 1996; Geider et al., 1998). In the acclimated state, the cellular concentration of LHCs allows phytoplankton to absorb enough light to nearly saturate the photosynthetic machinery but not absorbing so much to cause cellular damage. Consequently, the saturation irradiance for photosynthesis, I_k ($=P_{max}/a$), which is the inflection point in the photosynthesis-irradiance curve (Figure 18), co-varies with growth irradiance. While photosynthesis *per se* can not be related directly to total phytoplankton growth (Cullen, 1990), the modeling of phytoplankton acclimation to light, temperature and nutrients is closely linked to the modeling of photosynthesis vs. irradiance, because the chemical composition of phytoplankton is a strong function of growth conditions.

As light decreases exponentially with depth, photosynthesis for the majority of the water column is light-limited; however in surface waters light intensity can be sufficiently high to cause damage to the photo-

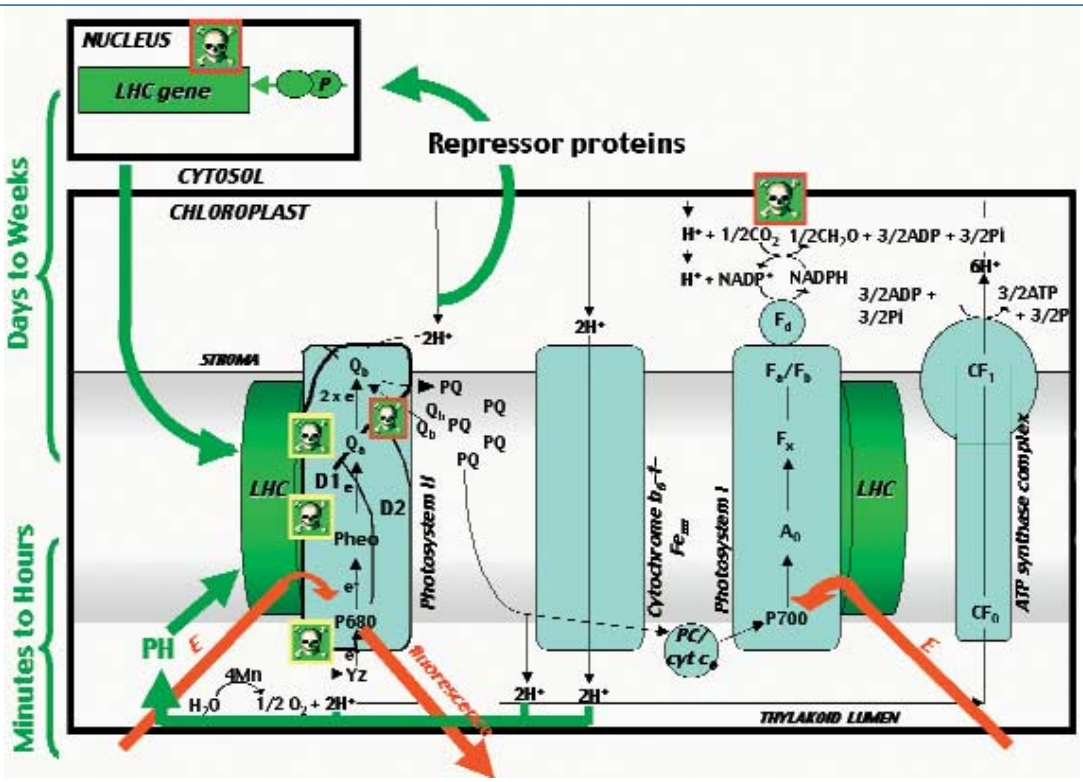

Figure 16. *The chemical reactions that convert radiant energy into chemical energy. A complete description of the light and dark reactions can be found in Falkowski and Raven (1998). The red arrows delineate the incoming light absorbed by the light harvesting complexes (LHCs) and the fluorescently emitted light by the phytoplankton. The absorbed light results in a stable charge separation and the electron is passed through a series of molecules, illustrated by the black arrows, with the net result being the formation of oxygen and organic carbon (CH_2O). The amount of CH_2O produced is dependent on the amount of light absorbed and the efficiency with which the absorbed radiation is utilized. The amount of light that is absorbed for photosynthesis is variable as the photosynthetically-active optical cross-section is adjusted by several different photo-acclimation processes (the green arrows). Over short time scales (minutes and hours), pigments can be inter-converted between photosynthetically-active and nonphotosynthetically-active pigments. Over longer time scales (days to weeks) pigment concentrations can be increased via nuclear-driven pigment synthesis. Both of these acclimation processes are coupled to the photosynthetically-induced pH gradient present across the thylakoid membrane (Demmig-Adams, 1990; Escoubas et al., 1995). The efficiency with which the absorbed light is utilized is impacted by the nutrient status of the cells, which provides the material to build the biochemical scaffolding required for photosynthesis. Secondarily, if visible and ultraviolet light radiation levels are excessive, the photosynthetic efficiency can be decreased from light-induced damage within the cell. The hypothesized target sites for visible (yellow outlined skulls) and ultraviolet (red outlined skulls) are delineated.*

synthetic machinery. The construction and repair of photo-damaged LHCs can be costly in terms of nitrogen and trace metals, therefore the dynamics of the LHCs, as well as overall cellular growth, are constrained by the availability of nutrients (cf. Falkowski and Raven, 1997). In optically deeper waters, the benefits of maximizing the cellular absorption are also constrained nutrient availability. However, in these waters there is also a secondary constraint caused by the decreasing absorption efficiency of the pigments in the LHCs as the cellular concentration of pigment increases, i.e. the "package effect" (Morel, 1990; Agusti, 1991). Thus, the optimization of LHCs by phytoplankton requires an internal mechanism that responds to nutrient and light availability over the time scale of cellular division.

Several other mechanisms, linked to the redox state of the thylakoid lumen, are used to regulate cellular light absorption (Figure 16). On short time scales (minutes), the photosynthetic cross section is adjusted by adding or removing pigments that dissipate the excitation energy as heat[2]. These rapidly reversible defenses (xanthophyll-cycling) 'down-regulate' the photosynthetic activity (Figure 19) in response to excess absorption of photosynthetically active radiation. This photo-protective capability is found in many phytoplankton. In Chl a-Chl c containing algae this involves the de-epoxidation of the pigment diadinoxanthin (DD) to diatoxanthin (DT; Demers et al., 1991). When light levels drop and the lumen pH increases, an epoxidase enzyme converts DT back to DD (Demmig-Adams, 1990; Owens et al., 1993). This xanthophyll cycling helps cells to minimize the build-up of oxidative radicals (often singlet oxygen) that cause lesions in the pho-

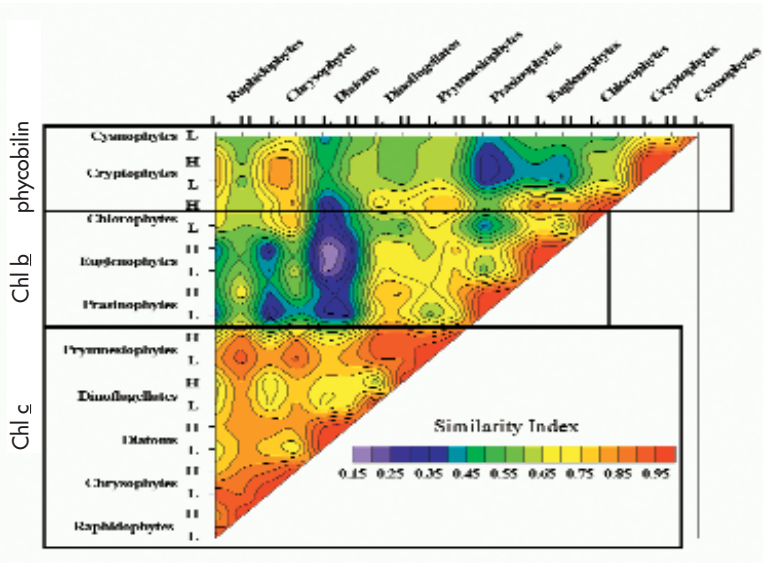

Figure 17. *Variability in the absorption spectra for different algal species. Similarity index values for comparisons of fourth-derivative transformations of absorption spectra among low (L) and high (H) light-acclimated cultures of the phylogenetic groups within chlorophyll (Chl) a/phycobilins (cyanobacteria, cryptophytes), Chl a/Chl b (chlorophytes, euglenophytes, prasinophytes), Chl a/Chl c/Fucoxanthin (raphidophytes, diatoms, chrysophytes), and Chl a/Chl c/Peridinin (dinoflagellates) spectral classes. The three major spectral classes are outlined with black boxes. Within each of the culture comparisons, the degree of similarity between absorption spectra was computed using a similarity index (SI) algorithm (Millie et al., 1997; Schofield et al., 1999; Kirkpatrick et al., 2000). Values of SI values will range from zero to one; as the two spectra approach equality, SI values approach one.*

tosynthetic machinery. These lesions cause decreases in the efficiency of photosynthesis and requires protein/pigment/enzyme synthesis to reverse the effects (Prasil et al., 1992; Critchley, 1994; Nickelsen and Rochaix, 1994). The target sites for the visible light damage are variable (Telfer and Barber, 1994); however, the majority of the damage sites are primary components to the photosystem complex II (PS II) (Figure 16).

On longer time scales (hours to weeks), cells can increase or decrease the number of LHCs per cell through a feedback process driven by the redox state of the plastoquinone (PQ) pool. Escoubas et al. (1995) describe an example of the nuclear-plastoquinone coupling regulating the creation and removal of LHCs. Here, nuclear transcription for LHC proteins were regulated by a negative feedback, as chlorophyll protein repressor factors were switched on when the redox potential of the PQ pool was reduced, causing LHC synthesis to declined as light intensity increased. This in essence provided the cells with a light meter for sensing and dynamically adjusting LHCs to changing levels of visible light. Optimization of the number of LHCs allows photosynthetic rates to be maximized and photo-damage rates to be minimized over the time scales of cellular division.

While surface populations of phytoplankton can reduce LHCs and expend more nutrient resources towards cellular division, rather than photochemical energy production, they are also exposed to ultraviolet radiation, which causes damage to cellular proteins and nucleic material. This damage reflects the physical disruption of biological molecules as opposed to the over-stimulated activity associated with visible light damage. The magnitude of the UV-induced damage is species-specific and is dependent on both dose and dosage rate (Jokiel and R. H. York, 1984; Karentz et al., 1991; Cullen and Lesser, 1991). On short time scales UV can depress photosynthetic rates and efficiencies (Figure 19); however perhaps more ecologically rele-

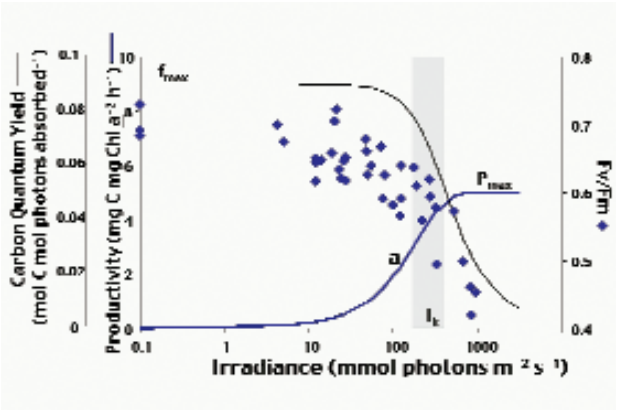

Figure 18. *Light-dependency of Chl-specific photosynthesis (bold blue line), the quantum yield for the carbon fixation (thin black line), and the maximum quantum yield for photosystem II activity (F_v/F_m, blue diamonds) for the red-tide dinoflagellate* Alexandrium fundyense *(Schofield et al., 1998). The parameters derived from the photosynthesis-irradiance curve (a, P_{max}, and I_k) are denoted. Both the carbon and photosystem II quantum efficiencies decrease dramatically when photosynthesis becomes light saturated.*

[2] The maximal photochemical conversion of light is about 35%, fluorescence ranges from 2 – 5%, and remainder is dissipated as heat (Falkowski and Raven, 1997).

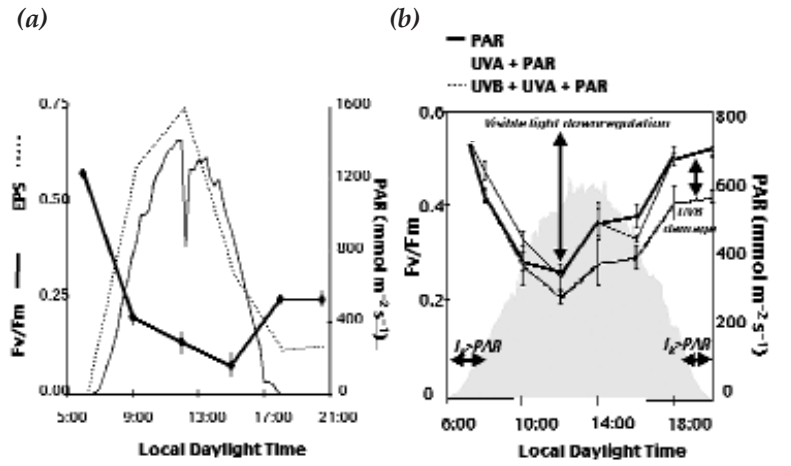

Figure 19. *Visible and ultraviolet light impact on photosynthetic quantum yields.* ***(a)*** *The diurnal pattern of the maximum quantum yield for photosystem II activity (F_v/F_m, bold line) and the epoxidation state (EPS = [diatoxanthin]/[diatoxanthin + diadinoxanthin], dotted line) for cultures of the toxic red tide dinoflagellate (formerly known as* Gymnodinium breve*) incubated under photosynthetically active irradiance (mmol quanta m^{-2} s^{-1}) (Evens et al., 2001). The diatinoxanthin is the photoprotective pigment which via the xanthophyll cycle converts to diadinoxanthin, the photosynthetically active form, under low light conditions. The increase in photoprotective pigments over the day is correlated with the midday decline in the photosynthetic efficiency of the phytoplankton;* ***(b)*** *Midday decline of the maximum quantum yield for photosystem II activity for frazil ice algae under the Antarctic ozone hole (Schofield et al., 1995). The different lines denote different incubators that selectively remove portions of the ultraviolet spectrum. Cells exposed to ultraviolet-B (UVB, dotted line) is significantly lower then cells not exposed to UVB radiation (bold and black lines). The gray shadow outlines the solar intensity over the day. The lower F_v/F_m values at the end of the day reflect UVB-induced damage to PSII.*

vant is that UV exposure over longer timescales leads an increasing number of mutations in DNA that can potentially be lethal (Vincent and Roy, 1993). The sensitivity to UV is related to the number and efficiency of the repair systems, production of UV sunscreens, and physical avoidance mechanisms (Karentz, 1994). Exposure to UV and visible light often leads to the enhancement of UV-sunscreens (also known as the mycosporine amino acids [MAAs]), (Sivalingham et al., 1974; Chiocarra et al., 1980; Tsujino et al., 1980; Dunlap and Chalker, 1986; Carreto et al., 1990) that confers a higher resistance to UV (Neale et al., 1998). The enhancement of MAAs is related to the light history of the cell and thus represents a dynamic process (Figure 20, Franklin et al., 2001). Release of MAAs to the water column via cell lysis or grazing is source of highly absorptive CDOM in high light environments (Vernet and Whitehead, 1996), although its importance to total CDOM absorption may be limited to extreme bloom conditions.

Optics and Ecological Processes

The earliest attempts to describe upper ocean ecology were focused on trying to predict fisheries yields, and it was assumed that phytoplankton were little more than the "grass in the blue pasture" of the ocean (Mills, 1989). Many of the ecologists trying to study and predict this blue pasture attempted to use terrestrial ecological theory to describe phytoplank-

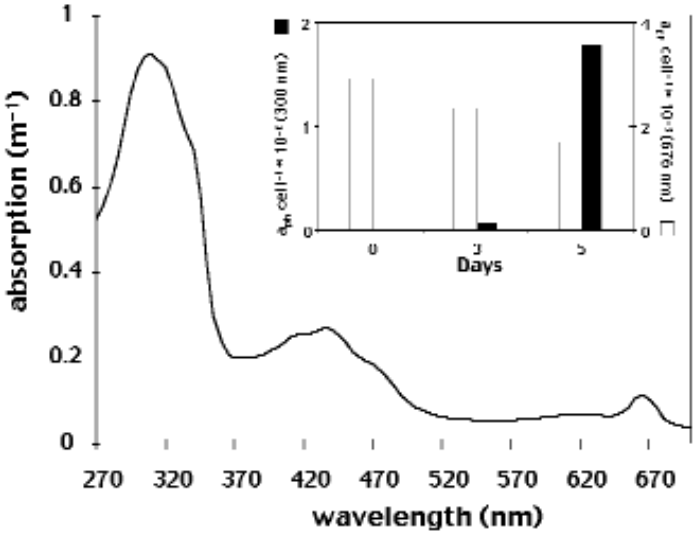

Figure 20. *An absorption spectrum collected on a methanolic extract of the toxic red-tide dinoflagellate* Karenia brevis *(formerly known as* Gymnodinium breve*) obtained during a nearshore bloom event in Sarasota Bay, Florida in February, 1995. The presence of significant microsporine amino acid absorption is common within positively-phototatic dinoflagellates (like* G. breve*), which are able to regulate their position in the water column. The concentration of MAAs can be rapidly increased when incident light levels increase (inset). The inset shows the increase in cellular MAAs absorption and decrease in cellular chlorophyll a absorption when the cultures incident light levels are doubled (from 150 to 300 mmol m^{-2} s^{-1}). Enhanced concentrations of MAAs can decrease UV-induced damage.*

ton growth. However, the large number of phytoplankton[3] seemed to defy the theory of competitive exclusion, which held that for stable environments with limited niches there should only be a few different species of organisms. This apparent paradox suggested that the ocean was far more variable than the simplifications ascribed to it (Hutchinson, 1961; Hobson, 1988), and that forecasting the change in ocean ecology may require forecasting the changes in individual phytoplankton populations.

For any given phytoplankton species, light harvesting abilities, light protecting abilities, and capabilities for vertical movement determine the optimal growth zone in the water column with respect to the downwelling solar energy (Cullen and MacIntyre, 1998; Schofield et al., 1999). This optical niche space within the water column is not invariant with respect to depth or season, but instead depends on the spectral distribution of the downwelling energy, the transmissivity of the over-lying water column, and the mixing rate of the phytoplankton within the sunlit waters, which can in calmer waters be overcome by swimming or buoyancy behavior (Cullen and MacIntyre, 1998). This optical niche space is commingled with nutrient and grazing niche spaces to yield a large continuum of different temporal and spatial habitats. Competitive success may hold for very short periods of time, e.g., blooms or red tides, but over longer time periods the constant variability of the physical, chemical, and optical environment results in spatially and temporally heterogeneous populations (Huisman and Weissing, 1999).

To quantitatively predict the ecological response of the upper ocean would require an approach that mathematically describes the change in phytoplankton population as a function of the time-dependent change in the environmental forcing. One of the first attempts to derive such functionality used the following simple differential equation as a starting point (Riley, 1946):

$$\frac{dP}{dt} = P\left(Ph - R - G\right) \qquad (1)$$

where time-dependent change in phytoplankton P was a function of the initial phytoplankton population, the photosynthetic rate, Ph, the respiration rate, R, and the grazing rate, G. Breaking this equation down into its component parts of photosynthesis (or production), respiration, and grazing would allow an ecologist to make individual controlled measurements, and apply these results to a formulation for each term. For example, photosynthesis could be described by cell growth or carbon fixation as a function of irradiance levels, e.g. through P vs. E relationships previously discussed. In addition, nutrients uptake and assimilation could be added to this equation as a non-linear function of the nutrient concentration (e.g. Dugdale, 1967; Droop, 1968) and the process of phytoplankton growth could be described as a minimization function of a limiting resource (Walsh, 1975):

$$P_h = P_{min}\left[\frac{V_m N}{K_N + N}, \frac{V_E E_z}{K_E + E_z}\right] \qquad (2)$$

where V_m is the maximum uptake of nutrients, N, and V_E is the maximum uptake of light energy at depth z, E_z, and the non-linear interactions between nutrients and light are described by Michaelis-Menten kinetic equations. The other terms of respiration and grazing losses in equation (2) can be described by similar non-linear formulations. As light decays exponentially with depth the light at a given depth E_z can be described with the function:

$$E_z = E_o e^{-kz} \qquad (3)$$

where E_0 is equal to the visible light energy (also called Photosynthetically Active Radiation [PAR]) at the sea surface, k is attenuation coefficient, and z is depth. This is the approach taken by Gordon Riley (1946) and its formulation, with minor adjustments, had been used for over fifty years to describe the propagation of light energy with depth. The phytoplankton stocks predicted by (1) were often accomplished in terms of chlorophyll a values, as this was a ubiquitous pigment to all phytoplankton and was relatively easy to measure. Thus, many early marine ecologists concentrated on measuring phytoplankton stocks and production as a function of the concentration of photosynthetic pigments.

Many of these earlier ecological studies focused on a limited number of spatial and temporal dimensions, i.e., integrating the differential equations for entire basins, or for seasonal cycles. This was done mainly to save computation time, as computer processing was a limiting factor in these studies. The results yielded by such simplified solutions were typically qualitatively similar to experimental results (Bissett et al., 1994), but were frequently in error because of inadequacies in resolving the physical and biological processes (Bissett et al., 1999). As computers speeds increased, so did the physical resolution of the models, such that 3-dimensional physical movement of water and its impacts on phytoplankton, nutrient, and grazer distributions could be directly calculated with the time-dependent phytoplankton calculations (Wroblewski et al., 1988; Walsh et al., 1989). When the physical circulation was adequately resolved these simulations frequently gave reasonable estimates of chlorophyll stocks and primary production.

[3] There are approximately 30,000 species of phytoplankton

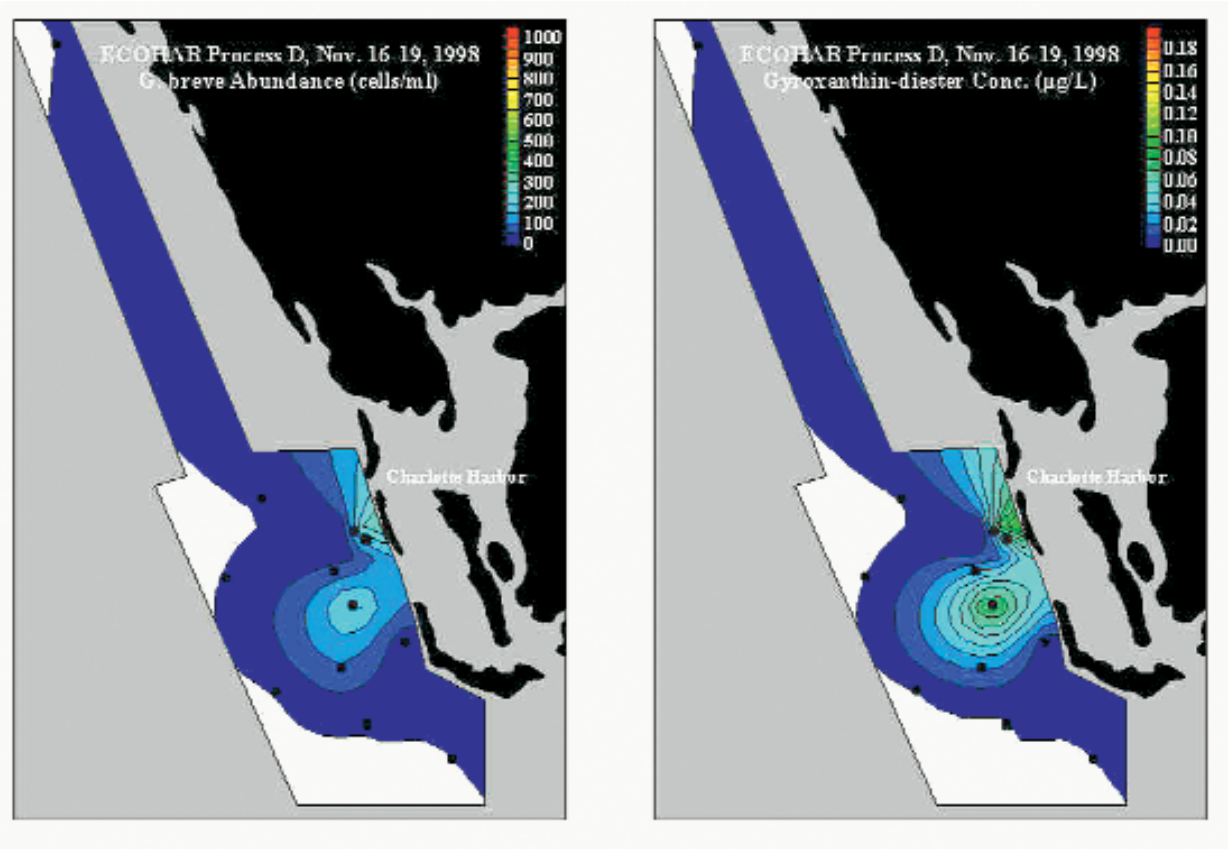

Figure 21. K. brevis *(formerly known as* G. breve*) abundance during ECOHAB process cruise November 1998 on the West Florida Shelf (courtesy G. Kirkpatrick, Mote Marine Laboratory).*

However, the ecological questions being asked of oceanographers were often difficult to describe in terms of pigment concentration alone. In addition to fisheries yields, oceanographers were also being asked biogeochemical questions regarding the cycling of greenhouse gases and the capacity of the ocean to draw down atmospheric CO_2 (SCOR, 1990). These questions required a better understanding of type of phytoplankton dominating the community assemblage, as well as the food web structure of the heterotrophic pyramid respiring the fixed carbon back to CO_2. While the measurement of total chlorophyll was easy, and there are physiological reasons (chlorophyll a is at the center of LHCs, thus visible energy processed by the photosystems could be related directly to carbon fixation) to normalize production as a function of chlorophyll (Cullen, 1990), chlorophyll a alone does not describe the process of carbon fixation and respiration by the upper ocean food web. For example, the ratio of organic carbon to chlorophyll in phytoplankton (C:Chl) can vary from about 10 to greater than 250 $g:g^{-1}$ (Cullen, 1990). Fortunately, models have been developed to predict C:Chl and to relate these changes directly to photosynthetic performance (Geider et al., 1998; Bissett et al., 1999a,b).

At the same time that computers began to achieve speeds that allowed for coarse resolution 3-dimensional studies, optical oceanography was given a global surveying tool in the form of the CZCS aboard the NIMBUS-7 satellite. This instrument provided the opportunity to synoptically sample broad swaths of the ocean, and relate the water-leaving radiance, L_w, to total chlorophyll (and its by-products) in the water. While there were wide error-bars on the retrieval of total chlorophyll from water, particularly near the coast, this sensor provided oceanographers with a visual scale of the ecological spatial and temporal variability. It also helped define the field of ocean color remote sensing.

The success of this early ocean color satellite has led to number of current and planned systems (Table 1) with varying spectral and spatial resolution. These data, combined with the development of *in situ* instrumentation (see article, this issue, by Maffione), has given oceanographers the ability to create ecological and optical time series with which to develop a wide variety of algorithms to determine surface water production and phytoplankton stocks on the basis of the color of the water (Campbell et al., 2001). These data and algorithms also allow for hypothesis testing on the impacts of physical forcing on the pigment structure of the water column. For example, upwelling should yield lower SST and inject greater nutrients to the euphotic

Table 1.
Suite of operational (or soon to be) ocean color sensors

Satellite/ Sensor	Country/ Channels	Data Rate (mps)	Delayed Resolution (km)	Real-Time Resolution (km)	Operational/ Launch	Revisit (days)/Time
EOS (2)	USA	13			OPL/2001	2/10:30
MODIS	2		0.25	0.25		
MODIS	5		0.5	0.5		2/13:30
MODIS	29		1.0	1.0		
NEMO	USA	150			2004	2/10:30
COIS	210		0.03	0.03		
Orbview-2	USA	13			OPL	12 hours
SeaWiFS	8		4	1.1		01:30/13:30
HY-1	China				2001	
COCTS	10	5.4	4	1		2/08:30
CZI	4		4	0.25		6/08:30
FYI C & D (2)	China	13			OPL/2001	12 hours
MVISR	10		4	1.1		9:00/18:00
IRS-P3	India	5.2	must be		OPL	2–5 days
MOS	13		turned on	0.2		
IRS-P4	India	10.4			OPL	2/12:00
OCM	8		1.8	0.36		
ADEOS-2	Japan	6			2001	2/10:45
GLI	6		1.0	0.25		
GLI	30		1.0	1.0		
POLDER	9(France)			6.5		
ENVISAT	ESA(Europe)	25			OCT 2001	2/?
MERIS	15		1.2	0.3		

zone, which in turn should yield greater biomass. This ecological result is seen optically by a change in the color of the water (Chavez, 1995; Dugdale et al., 1997). However, the same upwelling force will not always lead to the same level of primary production. The difference in source water supplies to the upwelling zones have a strong influence on phytoplankton biomass, so warmer and nutrient-poor upwelling during El Niño produces smaller responses (Chavez, 1996). The lesson is that while ocean color data and *in situ* optics could provide a measure of the ecological state of the water column at a given moment, a forecast of ecological structure and ocean color must be based on knowledge of circulation, ocean chemistry, and the larger-scale influences on their relationships.

The previous sections of this article suggest that the chemical and biological components of an ocean ecotone can be delineated by their optical properties. This, in turn, suggests that an ecological forecast, which incorporated the time-dependent change of the inherent optical properties of the optical constituents, could be remotely validated by optical measurements. Thus, accurate forecasting of the optical properties may provide a mechanism to assess the forecast's ensemble ecological accuracy, i.e. ecosystem structure and production. However, this would mean a dramatic increase in the level of complexity of the ecosystem modeling efforts previously described. Optical niches, as well as chemical and physical niches, would have to be explicitly described, and explicit numerical procedures formulated for the various phytoplankton species or functional groups to fill those niches.

The need to directly simulate different phytoplankton is also a biogeochemical necessity, as larger phytoplankton tended to have truncated food webs that yielded a greater flux of carbon to depth (Michaels and Silver, 1988; Legendre and Févre, 1989). The first of these efforts (e.g. Taylor et al., 1991) demonstrated the need for multiple groups in relation to the cycling of carbon. Further work suggested that differences in

(a)

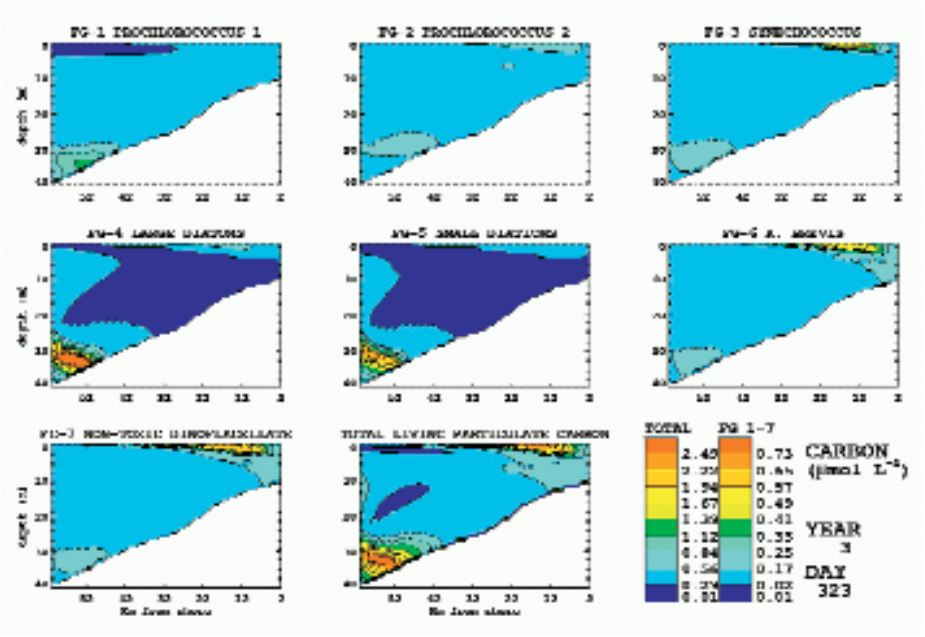

Figure 22. *EcoSim 2.0* K. brevis *Results for November 1998. This simulation was forced by a 2-dimensional flow calculation based on real winds during 1998 on the West Florida Shelf. Estuarine pulses of CDOM and nutrient were simulated to reflect the passage of Hurricanes Georges and Mitch.* ***(a)*** K. brevis *carbon stocks correspond to approximately* $3x10^5$ *cells liter*$^{-1}$ *(Bissett et al., 2001) and appear to match* K. brevis *cell counts and pigment stocks during that period (Figure 21);* ***(b)*** *the predicted Kd(412), Kd(487), and their ratio for the same day. The* K. brevis *populations are associated with a terrestrial CDOM and nutrient pulse.*

(b)

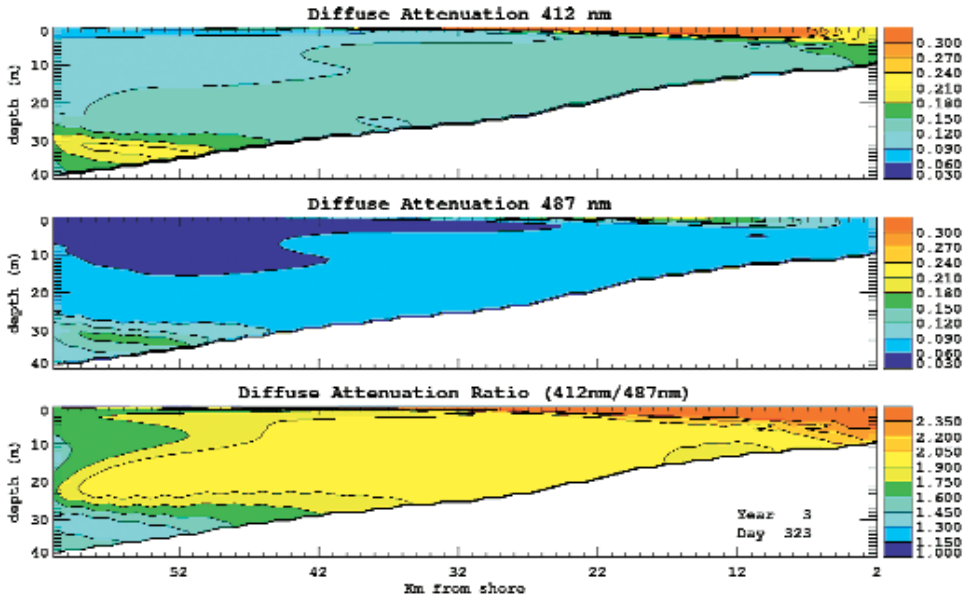

spectral irradiance at the sea surface could help separate different phytoplankton groups (Gregg and Walsh, 1992). However, the direct step to the prediction of inherent optical properties and their feedback into ecological structure has only recently been achieved (Bissett et al., 1999a,b). Recent efforts on the West Florida Shelf suggest that these types of models may be able to adequately resolve the ecological structure of different phytoplankton functional groups, where phytoplankton species are differentiated on size, pigment suites, nutrient uptake capabilities, growth rates, and grazing controls (Figures 21 and 22), and possibility predict the increased probability of a red tide occurrence.

This type of optical/ecological modeling expands the description of equations (2) and (3) to account for the different absorption properties of individual phytoplankton pigments and the differences in the spectral distribution of light. Thus, the efficiency of light harvesting by phytoplankton can be described as a function of the phytoplankton pigment suite and the ambient light field (Bissett et al., 1999a,b):

$$a_{ph\_i}(\lambda,z,t) = \sum \left\{ pigments_i(z,t)\left[mg \quad m^{-3}\right] \bullet a^*_{pig\_j}(\lambda)\left[m^2 \quad mg^{-1}\right] \right\} \quad (4)$$

where $a_{ph}(\lambda,z,t)$ is the absorption coefficient in (units of m^{-1}) of a phytoplankton functional group i, at depth z, and time t; pigments refers to the mass of pigments within the functional group at that time and location, and a^*_{pig} is the specific absorption of the pigment type. This absorption coefficient is used to determine the spectrally weighted absorption coefficient:

$$a^*_{ph}(z,t) = \frac{\int_{400}^{700} a_{ph}(\lambda,z,t)\ E_o(\lambda,z,t)\ d\lambda}{\int_{400}^{700} E_o(\lambda,z,t)\ d\lambda} \quad (5)$$

where $E_o(\lambda)$ refers to the scalar irradiance at a particular time and depth location. This spectrally weighted absorption coefficient is used to determine the slope of a P v. E curve for this phytoplankton functional group. As the phytoplankton pigment suite is allowed to change as a function of light and nutrient conditions, the value a^*_{ph} will also change, reflecting a feedback from the growth history of the functional group into its future fixation of inorganic carbon.

The feedback of phytoplankton growth into the ambient light field in these studies occurs via an approximation of the spectral downwelling irradiance. Similar in nature to equation (3), this approximation[4] takes a calculation of the absorption and scattering of all the optical constituents and derives a spectral downwelling diffuse attenuation coefficient for each depth (Morel, 1991):

$$K_d(\lambda,z) = \left[a_t(\lambda,z) + b_{bt}(\lambda,z)\right] / \bar{\mu}_d(\lambda,z) \quad (6)$$

where $a_t(\lambda,z)$ and $b_{bt}(\lambda,t)$ are the sum total of all physical, chemical, and biological absorption and backscattering, and $\bar{\mu}_d(\lambda,z)$ is an estimate of the geometrical structure of the light field. This estimate of the downwelling diffuse attenuation is used in:

$$E_d(\lambda,z) = E_d(\lambda,0^-) \cdot \exp\left[\int_{0^-}^{z} K_d(\lambda,z)\, dz\right] \quad (7)$$

where $E_d(\lambda,0^-)$ refers to the spectral distribution of light just below the sea surface. $E_d(\lambda,z)$ is then used to approximate the scalar irradiance $E_o(\lambda,z)$, and thus closing the loop between optical prediction of the light field and the biological processes. Similar spectral equations can be derived to describe the changes in the other optical constituents, e.g., CDOM. Coupling these optical equations with other non-linear equations to describe the biological response to physical and chemical forcing establishes a complex numerical ecosystem that is designed to represent the oceanic ecosystem. The future of these studies will be found in a truly dynamic ecological numerical simulation, where the biologically forced spectral attenuation coefficients would be used to simulate a physical response to heat flux and the establishment of the MLD, thereby impacting future nutrient fluxes and the vertical phytoplankton positioning

There is much debate about the veracity of the results from such complex simulations. It was often found that more simple, non-linear models degenerated into chaotic solutions when their parameters were adjusted to ecologically unreasonable setting (May, 1971; May, 1974). In addition, simple models that predicted only production and chlorophyll could be tuned to match many of the oceanographic datasets, but had little forecasting ability. The studies by Bissett et al. (1999a) suggested that increased complexity reduces the parameter tuning because of the larger number of validation variables that must be matched. Rather than matching only production and chlorophyll *in situ* data sets, these complex simulations are validated against biogeochemical data set of total pigments, cell counts, ammonium, nitrate, silicate, phosphate, dissolved inorganic carbon, CDOM, organic particle fluxes, as well as optical data sets of absorption, scattering, remote sensing reflectance. In addition, recent ecological work suggests that ecosystem complexity is itself a stabilizing factor (Hulot et al., 2000). Thus, forecasting the optical condition of the blue pasture may require directly addressing the complexity of the ecological relationships between light, physics, biology, and chemistry.

[4] An exact solution to the Radiative Transfer Equation (RTE) is possible, but numerically more complicated (Mobley, 1994). These equations are meant to illustrate a numerical connection between simulated inherent optical properties and apparent optical properties..

Where Do We Go From Here?

The previous sections are discussions of what we know about the link between optical processes and the physical, chemical, and biological components of upper ocean ecology. In the final section a quantitative link between ecological processes and optics that incorporates feedback reactions among the components was discussed. These discussions outline the research between optics and their respective fields. Where we go from here depends in a large part on the science questions being asked. The global issues of climate change and human-induced impacts on oceanic systems are certainly larger than any one scientific discipline. It also appears that predicting water color and clarity for a specific location is nearly as complicated as attempting to solve global biogeochemical issues. However, these issues may not be as intractable as they appear.

Forecasting the ocean environment requires a coupled observation/modeling system with which to test and develop our numerical abilities. One approach to developing a predictive system would be to start at small scale, and then expand outwards as resources and tools became available. This system would have to be large enough to be biogeochemical relevant, but small enough to be computationally and observationally feasible. A shelf-wide observing system that can sample and, with assimilative models, forecast the physical, chemical, biological, and optical regimes of the near-shore environment is being developed in the New York Bight (NYB). The New Jersey (NJ) Shelf Observing System (SOS), (Glenn et al., 2001; Schofield et al., 2001) is a regional expansion of Rutgers' existing local-scale Long-term Ecosystem Observatory (LEO) (Glenn et al., 2001; Schofield et al., 2001) located offshore the Jacques Cousteau National Estuarine Reserve. NJ-SOS, in combination with the Gulf of Maine Ocean Observing System (GoMOOS) are the shelf-scale cornerstones of the recently formed NorthEast Observing System (NEOS), a consortium of all the major oceanographic institutions in the northeast. The current national plan calls for a federation of regional coastal observatories such as NEOS to jumpstart the coastal component of the Global Ocean Observing System (GOOS).

NJ-SOS components currently include: (1) direct access to a growing number of satellite platforms; (2) long-range, intermediate-range, and bistatic Coastal HF Radar systems that measure real-time surface currents up to 200 km offshore; (3) strategically placed, long duration physical/bio-optical moorings and cabled observatories for subsurface time series at fixed locations; (4) research vessels available for adaptive physical, bio-optical and chemical sampling; and (5) a fleet of long-duration glider-type Autonomous Underwater Vehicles (AUVs) for mobile subsurface physical-/bio-optical observations. NJ-SOS will further provide the data stream for the new generation of data-assimilative ocean nowcast/forecast ocean models. The Terrain-following Ocean Modeling System (TOMS) is being developed by the U.S. Office of Naval Research to be an expert ocean modeling system for scientific and operational applications. The TOMS model, which supports advanced data assimilation strategies, is coupled with operational atmospheric models, supports massive parallel computations, and provides a re-locatable model with a common set of options for all coastal developers. The TOMS model is being coupled to the Ecological Simulator (EcoSim). The EcoSim model, also being developed by the Office of Naval Research, simulates the hyperspectral bio-optical properties of the water column via a size-fractionated phytoplankton community, including the optical constituents of labile and recalcitrant colored dissolved organic matter. EcoSim utilizes the spectral distribution of light energy, along with temperature and nutrients, to drive the growth of phytoplankton functional groups (FG) representing broad classes of the phytoplankton species, as well as the cycling of biogeochemical elements of carbon, nitrogen, silica, phosphorous, and iron. The advantage of the EcoSim model is that it allows for direct simulation of the inherent optical properties (IOPs), which can be used to directly simulate the hyperspectral upwelling radiance field. Thus, validation is accomplished via the data stream provided by remote sensing platforms, rather than by derived products.

Developing such an *in situ* observation system for all of the world's oceans would be difficult. However, a validated set of physical, chemical, biological, and optical models could be extended globally. In this case, optics provides a globally unifying mechanism to sample and describe the ecological state of the ocean. In particular, hyperspectral remote sensing data could be used to ascertain the current ecological structure of a non-accessible region of the world. This information, coupled with other remote sensing data stream such as autonomous profiling radiometers, SST, sea surface height, and sea surface roughness, could be used to drive a coupled physical, chemical, biological, and optical simulation that could then be validated against future hyperspectral data collection. In this nowcast/forecast scenario, future global ocean biogeochemical fluxes could be determined with an ever expanding remotely sensed observation and modeling system.

The fields of ocean optics and ecology are inextricably inter-twined, and they cannot be adequately studied *in vacuo*. However, supply of energy from the sun, its photochemical transformation, and its re-radiation to space can be used for integrated physical, chemical, biological, and optical studies to address the state of the oceans, and forecast its future.

Box 1

Inherent Optical Properties (IOPs)

The IOPs are the fundamental optical properties of the medium itself (i.e. the seawater and suspended and dissolved materials within it). They do not depend on the nature of the ambient light field. IOPs measured *in situ* and in the lab from the same sample of water would be identical. IOPs are typically measured as a function of the depth z and the wavelength of light λ. The most commonly used IOPs are defined below.

$a(z, \lambda)$ = absorption coefficient

Absorption refers to the conversion of radiant (light) energy into other forms such as chemical or thermal. In a beam of light, the fraction of power absorbed per unit distance of travel is called the absorption coefficient; its units are 1/m.

$b(z, \lambda)$ = scattering coefficient

Scattering refers to a change in direction of light. The scattering coefficient is the fraction of power in a beam of light that is scattering into a new direction, per unit distance of travel; its units are 1/m.

$c(z, \lambda)$ = attenuation coefficient

Attenuation refers to the loss of power from a beam of light owing to both absorption and scattering. The attenuation coefficient c is the sum of a and b.

$\tilde{\beta}(\psi)$ = scattering phase function

The scattering angle ψ is the direction of the scattered light, measured from 0 in the initial (unscattered) direction. The scattering phase function $\tilde{\beta}(\psi)$ describes how much light is scattered into a small solid angle in direction ψ; its units are 1/sr. (Solid angle, with units of steradian (sr), is a three-dimensional generalization of the plane angle, measured in radians.)

If the IOPs a, b, and $\tilde{\beta}(\psi)$ are known, it is possible to predict how light will behave in the medium.

Radiometric Properties

The IOPs describe the medium; the radiometric properties describe the light. The radiance $L(z, \lambda, \theta, \phi)$ describes how much light is going in a particular direction (θ, ϕ) at each location (z) and wavelength (λ). The full radiance distribution is seldom measured. Irradiances are integrals of the radiance over various directions (e.g., upward or downward). The commonly measured irradiances are as follows:

$E_d(z, \lambda)$, $E_u(z, \lambda)$ = downwelling and upwelling plane irradiance

E_d (E_u) is a weighted integral of radiance over the downward (upward) hemisphere of directions; E_d (E_u) gives the power per unit area traveling downward (upward) across a horizontal surface at depth z. The net irradiance $E = E_d - E_u$ gives the net flow of power across a horizontal surface.

$E_{od}(z, \lambda)$, $E_{ou}(z, \lambda)$ = downwelling and upwelling scalar irradiance

These are unweighted integrals of radiance over downward and upward directions; the sum $E_o = E_{od} + E_{ou}$ is proportional to the energy density (energy per unit volume) of the light field.

Apparent Optical Properties (AOPs)

The light field in a water body (i.e., the radiometric properties) is determined by both the IOPs and the incident lighting conditions (e.g., the solar elevation and atmospheric conditions). However, the connections between the IOPs, the incident lighting, and the radiance and irradiances are complicated. The irradiances can change magnitude quickly, for example if the sun goes behind a cloud, even though the IOPs were unchanged. AOPs are intended to give approximate but more stable measures of the light field, which in turn can be related to the IOPs. AOPs are always a ratio of radiometric variables; they can be measured only *in situ*. Some of the commonly used AOPs are defined as follows:

$R(z, \lambda) = E_u(z, \lambda) / E_d(z, \lambda)$

The irradiance reflectance is the ratio of the upwelling to the downwelling plane irradiance; nondimensional.

$R_{rs}(\lambda) = L_w(\text{in air}, \lambda) / E_d(\text{in air}, \lambda)$

The remote-sensing reflectance is the ratio of the water-leaving radiance L_w to the incident irradiance; both quantities are measured in air, just above the sea surface; units of 1/sr.

$T(z, \lambda) = E_d(z, \lambda) / E_d(\text{in air}, \lambda)$

The spectral transmission function relates the net irradiance at depth z to the incident downwelling irradiance just above the sea surface; nondimensional. The transmission function includes the effects of both sea surface reflectance and reflectance by the water itself.

$K_x(z, \lambda) = - d/dz [\ln E_x(z, \lambda)]$

The diffuse attenuation coefficients are a measure of the rate of decay with depth of downwelling (x=d), upwelling (x=u) and scalar (x=o) irradiance; units of 1/m.

Acknowledgements

This work was funded by the U.S. Office of Naval Research.

References

Agusti, S., 1991: Allometric scaling of light absorption and scattering by phytoplankton cells. *Can. J. Fish. Aquat. Sci.,* 48, 763–768.

Andreae, M.O. and R.J. Ferek, 1992: Photochemical production of carbonyl sulfide in seawater and its emission to the atmosphere. *Global Biogeochemical Cycles,* 6, 175–183.

Arrigo, K.R. and C.W. Brown, 1996: Impact of chromophoric dissolved organic matter on UV inhibition of primary productivity in the sea. *Marine Ecology Progress* Series, 140, 207–216.

Benner, R. and B. Biddanda, 1998: Photochemical transformations of surface and deep marine dissolved organic matter: Effects on bacterial growth. *Limn. and Oceanogr.,* 436, 1373–1378.

Bidigare, R.R., J.H. Morrow and D.A. Kiefer, 1989: Derivative analysis of spectral absorption by photosynthetic pigments in the western Sargasso Sea. *J. Mar. Res.,* 47, 323–341.

Bissett, W.P., K.L. Carder, J.J. Walsh and D.A. Dieterle, 1999: Carbon cycling in the upper waters of the Sargasso Sea: II. Numerical simulation of apparent and inherent optical properties. *Deep-Sea Res.,* 462, 271–317.

Bissett, W.P., M.B. Meyers, J.J. Walsh and F.E. Muller-Karger, 1994: The effects of temporal variability of mixed layer depth on primary productivity around Bermuda. *J. Geophys. Res.,* 99C4, 7539–7553.

Bissett, W.P., J.J. Walsh, D. Dieterle, J. Jolliff, S. Lohrenz, O. Schofield, G. Kirkpatrick, R.A. Arnone, G. Vargo, C. Heil, R.H. Weisberg and F.E. Muller-Karger, 2001: Predicting ecology, optics, and red tides on the West Florida Shelf, in preparation.

Bissett, W.P., J.J. Walsh, D.A. Dieterle and K.L. Carder, 1999: Carbon cycling in the upper waters of the Sargasso Sea: I. Numerical simulation of differential carbon and nitrogen fluxes. *Deep-Sea Res. I,* 462, 205–269.

Blough, N.V. a. R.G.Z., 1995: Reactive oxygen species in natural waters. In: *Active Oxygen in Chemistry.* J. S. V. C. S. Foote, A. Greenberg, and J. F. Liebman, Chapman and Hall, New York, 280–333.

Boss, E., W.S. Pegau, J.R.V. Zaneveld and A.H.B. Barnard, 2001: Spatial and temporal variability of absorption by dissolved material at a continental shelf. *J. Geophys. Res.,* 106C5, 9499–9507.

Brocks, J.J., G.A. Logan, R. Buick and R.E. Summons, 1999: Archean molecular fossils and the early rise of eukaryotes. *Science,* 285, 1033–1036.

Broecker, W.S. and T. Takahashi, 1985: Sources and flow patterns of deep-ocean waters as deduced from potential temperature, salinity, and initial phosphate concentration. *J. Geophys. Res.,* 90C4, 6925–6939.

Butler, W.L. and D.W. Hopkins, 1970: An analysis of fourth derivative spectra. *Photochem. Photobiol.,* 12, 451–456.

Campbell, J.W. and et al., 2001: Comparison of algorithms for estimating ocean primary productivity from surface chlorophyll, temperature, and irradiance. *Glob. Biogeochem. Cycles,* submitted.

Carreto, J.I., M.O. Carignan, G. Daleo and S.G. DeMarco, 1990: Occurrence of mycosporine-like amino acids in the red tide dinoflagellate *Alexandrium excavatum* UV-absorbing compounds. *J. Plankt. Res.,* 12, 909–921.

Chavez, F.P., 1995: A comparison of ship and satellite chlorophyll from California and Peru. *J. Geophys. Res.,* 100(24), 855–24, 862.

Chavez, F.P., 1996: Forcing and biological impact of onset of the 1992 El Niño in central California. *Geophys. Res. Letters,* 23, 265–268.

Chen, Y., S.U. Khan and M. Schnitzer, 1978: Ultraviolet irradiation of dilute fulvic acid solutions. *Soil Sci. Soc. Am. J.,* 42, 292–296.

Chiocarra, F., A.D. Gala, M.D. Rosa, E. Noveliio and G. Prota, 1980: Mycosporine amino acids and related compounds from the eggs of fishes. *Bull. Soc. Chim. Belg.,* 89, 1101–1106.

Critchley, C., 1994: D1 protein turnover: response to photodamage or regulatory mechanism? Photoinhibition of photosynthesis from molecular mechanisms to the field. N.R. a. J.R.B. Baker. Oxford, BIOS Scientific Publ., 195–201.

Cullen, J.J., 1990: On models of growth and photosynthesis in phytoplankton. Deep-Sea Res., 374, 667–683.

Cullen, J.J. and J.G. MacIntyre, 1998: Behavior, physiology and the niche of depth-regulating phytoplankton. *Physiological Ecology of Harmful Algal Blooms.* D.M. Anderson, A.D. Cembella and G.M. Hallegraeff, Springer-Verlag, New York, 559–580.

Cullen, J.J. and M.P. Lesser, 1991: Inhibition of photosynthesis by ultraviolet radiation as a function of dose and dosage rate: results for a marine diatom. *Mar. Bio.,* 111, 183–190.

Darwin, C., 1988: *Charles Darwin's Beagle Dairy.* Cambridge University Press, Great Britain.

DeGrandpre, M.D., A. Vodacek, R.K. Nelson, E.J. Bruce and N.V. Blough, 1996: Seasonal seawater optical properties of the U.S. Middle Atlantic Bight. *J. Geophys. Res.,* 101C10, (22), 727–22736.

Del Castillo, C.E. and P.G. Coble, 2000: Seasonal variability of the colored dissolved organic matter during the 1994-95 NE and SW Monsoons in the Arabian Sea. *Deep-Sea Res. II,* 477-8, 1563–1579.

Del Castillo, C.E., F. Gilbes, P.B. Coble and F.E. Muller-Karger, 2000: On the dispersal of riverine colored dissolved organic matter over the West Florida Shelf. *Limn. Oceanogr.* 456, 1425–1432.

Delwiche, C.E. 1999: Tracing the thread of plastid diversity through the tapestry of life. *Amer. Nat.,* 154, S164–S177.

Demers, S., S. Roy, R. Gagnon and C. Vignault, 1991: Rapid light-induced changes in cell fluorescence and in xanthophyll-cycle pigments of *Alexandrium excavatum* Dinophyceae and *Thalassiosira pseudonana* Bacillariophyceae: a photo-protection mechanism. *Mar. Ecol. Prog. Ser.,* 76, 185–193.

Demmig-Adams, B., 1990: Carotenoids and photoprotection: A role for the xanthophyll zeaxanthin. *Biochim. Biophys. Acta.,* 1020, 1–24.

Droop, M.R., 1968: Vitamin B_{12} and marine ecology. IV. The kinetics of uptake, growth and inhibition in *Monochrysis lutheri. J. Mar. Bio. Ass. U.K.,* 48, 689–733.

Dugdale, R.C., 1967: Nutrient limitation in the sea: dynamics, identification, and significance. *Limn. Oceanogr.,* 12, 685–695.

Dugdale, R.C., C.O. Davis and F.P. Wilkerson, 1997: Assessment of new production at the upwelling center at Point Conception, California, using nitrate estimated from remotely sensed sea surface temperature. *J. Geophys. Res.,* 102C4, 8573–8601.

Dunlap, W.C. and B.E. Chalker, 1986: Identification and quantitation of near-UV absorbing compounds S-320 in a hermatypic scleractinian. *Coral Reefs,* 5, 1–5.

Escoubas, J.-M., M. Lomas, J. LaRoche and P.G. Falkowski, 1995: Light intensity regulation of *cab* gene transcription is signaled by the redox state of the plastoquinone pool. *Proc. Nat. Acad. Sci. USA,* 92, 10237–10241.

Evens, T.J., G.J. Kirkpatrick, D.F. Millie, D. Chapman and O. Schofield, 2001. Xanthophyll-cycling and photophysiological regulation of *Gymnodinium breve* in response to fluctuating natural irradiance. *J. Plank. Res.,* in press.

Falkowski, P.G. and J. LaRoche, 1991: Acclimation to Spectral Irradiance in Algae. *J. Phycol.,* 27, 8–14.

Falkowski, P.G. and J.A. Raven, 1997: *Aquatic Photosynthesis.* Blackwell Sciences, Inc., Malden, Massachusetts.

Franklin, L.A., G. Krabs and R. Kuhlencamp, 2001: Blue light and UV-A radiation control the synthesis of mycosporine-like amino acids in *Chondrus crispus florideophyceae. J. Phycol.,* 37, 257–270.

Gao, H. and R.G. Zepp, 1998: Factors influencing photoreactions of dissolved organic matter in a coastal river of the southeastern United States. *Environ. Sci. Tech.,* 32, 2940–2946.

Geider, R.J., H.L. MacIntyre and T.M. Kana, 1996: A dynamic model of photoadaptation in phytoplankton. *Limn. Oceanogr,* 411, 1–15.

Geider, R.J., H.L. MacIntyre and T.M. Kana, 1998: A dynamic regulatory model of phytoplanktonic acclimation to light, nutrients, and temperature. *Limn. Oceanogr.,* 434, 679–694.

Glenn, S.M., O. Schofield, R.E. Chant and G.J.F., 2001: The New Jersey Shelf Observing System. *Oceanology,* in press.

Graneli, W., M. Lindell and L. Tranvik, 1996: Photo-oxidative production of dissolved inorganic carbon in lakes of different humic content. *Limn. Oceanogr.,* 414, 698–706.

Gregg, W.W. and J.J. Walsh, 1992: Simulation of the 1979 spring bloom in the Mid-Atlantic Bight: A coupled physical/biological/optical model. *J. Geophys. Res.,* 97C4, 5723–5743.

Grzybowski, W., 2000: Effect of short-term irradiation on absorbance spectra of chromophoric organic matter dissolved in coastal and riverine water. *Chemosphere,* 4012, 1313–1318.

Hobson, L.A., 1988: Paradox of the phytoplankton—an overview. *Biological Oceanography,* 6, 493-504.

Huisman, J. and F.J. Weissing, 1999: Biodiversity of plankton by species oscillations and chaos. *Nature,* 402, 407–410.
Hulot, F.D., G. Lacroix, F. Lescher-Moutoue and M. Loreau, 2000: Functional diversity governs ecosystem response to nutrient enrichment. *Nature,* 405, 340–344.
Hutchinson, G.E., 1961: The paradox of the plankton. *Am. Naturalist.,* XCV882, 137–145.
Johnsen, G., N.B. Nelson, R.V.M. Jovine and B.B. Prézelin, 1994: Chromoprotein- and pigment-dependent modeling of spectral light absorption in two dinoflagellates, *Prorocentrum minimum and Heterocapsa pygmaea. Marine Ecology Progress Series,* 114, 245–258.
Jokiel, P.L. and J.R.H. York, 1984: Importance of ultraviolet in photoinhibition of microbial growth. *Limn. Oceanogr.,* 29, 192–199.
Kahru, M. and B.G. Mitchell, 2001: Seasonal and nonseasonal variability of satellite-derived chlorophyll and colored dissolved organic matter concentration in the California *Current.* 106, C22517–2529.
Kantha, L.H. and C.A. Clayson, 1994: An improved mixed layer model for geophysical applications. *J. Geophys. Res.,* 99C12, 25, 235–25,266.
Karentz, D., 1994: Ultraviolet tolerance mechanisms in Antarctic marine organisms. Ultraviolet Radiation in Antarctica: Measurements and Biological Effects. S.a.P. Weiler, P., *Ant. Res. Ser.,* 62, 93–111.
Karentz, D., J.E. Cleaver and D.L. Mitchell, 1991: Cell survival characteristics and molecular responses of Antarctic phytoplankton to ultraviolet-B. *J. Phycol.,* 27, 326–341.
Kirk, J.T.O., 1994: *Light and Photosynthesis in Aquatic Ecosystems.* Cambridge, University Press.
Kirkpatrick, G., D.F. Millie, M.A. Moline and O. Schofield, 2000: Absorption-based discrimination of phytoplankton species in naturally mixed populations. *Limn. Oceanogr.,* 42, 467–471.
Kotzias, D., A. Herrmann, A. Zsolnay, H. Russi and F. Korte, 1986: Photochemical reactivity of humic materials. *Naturwissenschaften,* 73, 35–36.
Kraus, E.B. and J.A. Businger, 1994: *Atmosphere-Ocean Interaction.* Oxford University Press, New York, 362.
Kuhnle, J.A., R.E. Lundin and A.C. Waiss, 1972: Photodecarboxylation of dicarboxylic acids in the presence of ironIII chloride. *J. Am. Chem. Soc. Chem. Commun.,* 1, 287–288.
Kuwahara, V.S., H. Ogawa, T. Toda, T. Kikuchi and S. Taguchi, 2000: Variability of bio-optical factors influencing the seasonal attenuation of ultraviolet radiation in temperate coastal waters of Japan. *Photochem. Photobiol.,* 72(2), 193–199.
Legendre, L. and J.L. Févre, 1989: *Hydrodynamical singularities as controls of recycled versus export production in oceans.* Wiley, Chichester, England.
Letelier, R.M., D.M. Karl, M.R. Abbott, P. Filament, M. Freilich, R. Lukas and T. Strub, 2000: Role of late winter mesoscale events in the biogeochemical variability of the upper water column of the North Pacific Suptropical Gyre. *J. Geophys. Res.,* 10512, 28723–28739.
Lewis, M.R., 1987: Phytoplankton and thermal structure in the tropical ocean. In: *Oceanologica Acta,* Proceedings International Symposium on Equatorial Vertical Motion, 6-10 May 1985, Paris.
Lewis, M.R., M.E. Carr, G.C. Feldman, W. Esais and C. McClain, 1990: Influence of penetrating solar radiation on the heat budget of the equatorial Pacific Ocean. *Nature,* 347, 543–545.
Li, J.W., Z. Yu, G.M.L. Zhang, X. Cai and Chao, 1996: Effect of ultraviolet irradiation on the characteristics and trihalomethanes formation potential of humic acid. *Water Research,* 30, 347–350.
Lorenzen, C.J., 1972: Extinction of light in the ocean by phytoplankton. *J. Cons. Int. Explor. Mer.,* 34, 262–267.
Maxwell, D.P., S. Falk and N.P.A. Huner, 1995: Photosystem II excitation pressure and development of resistance to photoinhibition. *Pl. Physiol.,* 107, 687–694.
Maxwell, D.P., S. Falk, C.G. Trick and N.P.A. Huner, 1994: Growth at low-temperature mimics high-light acclimation in *Chlorella- vulgaris. Pl. Physiol.,* 105, 535–543.
May, R.M., 1971: Stability in multispecies community models. *Mathematical Biosci.,* 12, 59–79.
May, R.M., 1974: *Stability and Complexity in Model Ecosystems. Princeton,* Princeton University Press.
Michaels, A.F. and M.W. Silver, 1988: Primary production, sinking fluxes and the microbial food web. *Deep-Sea Res.,* 354, 473–490.
Miller, W.L., 1994: *Recent advances in the photochemistry of natural dissolved organic matter. Aquatic and Surface Photochemistry.* G.R. Helz, Lewis Publishers, Boca Raton, 111–128.
Miller, W.L. and M.A. Moran, 1997: Interaction of photochemical and microbial processes in the degradation of refractory dissolved organic matter from a coastal marine environment. *Limn. Oceanogr,* 42(6), 1317–1324.
Miller, W.L. and R.G. Zepp, 1995: Photochemical production of dissolved inorganic carbon from terrestrial organic matter: Significance to the oceanic organic carbon cycle. *Geophys. Res. Letters,* 22(4), 417–420.
Millie, D.F., G.J. Kirkpatrick and B.T. Vinyard, 1995: Relating photosynthetic pigments and in vivo optical density spectra to irradiance for the Florida red-tide dinoflagellate *Gymnodinium breve. Marine Ecology Progress Series,* 120, 65–75.
Millie, D.F., O. Schofield, G.J. Kirkpatrick, G. Johnsen, P.A. Tester and B.T. Vinyard, 1997: Phytoplankton pigments and absorption spectra as potential 'Biomarkers' for harmful algal blooms. A case study of the Florida red-tide dinoflagellate, *Gymnodinium breve. Limn. Oceanogr.,* 42, 1240–1251.
Mills, E.L. 1989. *Biological Oceanography: An Early History, 1870-1960.* Cornell University Press, Ithaca, New York.
Mitchell, B.G., 1994: Coastal zone color scanner restrospective. *J. Geophys. Res.,* 99C4, 7291–7292.
Mobley, C.D., 1994: *Light and Water.* Academic Press, San Diego, California.
Moore, R.M. and O.C. Zafiriou, 1994: Photochemical production of methyl iodide in seawater. *J. Geophys. Res.,* 99, 16415–16420.
Mopper, K. and D.J. Kieber, 2000: *Marine photochemistry and its impact on carbon cycling.* The effects of UV radiation in the marine environment. S.D. Mora, S. Demers and M. Vernet. Cambridge University Press, Cambridge, 101–129.
Mopper, K., X. Zhou, R.J. Kieber, D.J. Kieber, R.J. Sikorski and R.D. Jones, 1991: Photochemical degradation of dissolved organic carbon and its impact on the oceanic carbon cycle. *Nature,* 353, 60–62.
Moran, M.A. and R.E. Hodson, 1994: Support of bacterioplankton production by dissolved humic substances from three marine environments. *Marine Ecology Progress Series,* 110, 241–247.
Moran, M.A., W.M. Sheldon and R.G. Zepp, 2000: Carbon loss and optical property changes during long-term photochemical and biological degradation of estuarine dissolved organic matter. *Limn. Oceanogr.,* 45(6), 1254–1264.
Moran, M.A. and R.G. Zepp, 1997: Role of photochemistry in the formation of biologically labile compounds from dissolved organic matter. *Limn. Oceanogr,* 42: 1307–1316.
Morel, A., 1990: *Optics of marine particles and marine optics: Particle analysis in oceanography.* S. Demers. Springer-Verlag, New York, 141–188.
Morel, A., 1991: Light and marine photosynthesis: A spectral model with geochemical and climatological implications. *Progress in Oceanography,* 26, 263–306.
Morel, A. and D. Antoine, 1994: Heating rate within the upper ocean in relation to its bio-optical state. *J. Phys. Oceanogr.,* 24, 1652-1655.
Murtugudde, R., J. Beauchamp and A.J. Busalacchi, 2001: Effects of penetrative radiation on the upper tropical ocean circulation. *J. Climate,* in press.
Nelson, J.R. and S. Guarda, 1995: Particulate and dissolved spectral absorption on the continental shelf of the southeastern United States. *J. Geophys. Res.,* 100C5, 8715–8732.
Nelson, N.B., D.A. Siegel and A.F. Michaels, 1998: Seasonal dynamics of colored dissolved material in the Sargasso Sea. *Deep-Sea Res.,* 45(6), 931–957.
Nickelsen, J. and J.D. Rochaix, 1994: Regulation of synthesis of D1 and D2 proteins of photosystem II: Photoinhibition of Photosynthesis from Molecular mechanisms to the Field. In: *BIOS Scientific Publ.,* N.R. Baker, Bowyer J.R., Oxford, 179–190.
Nieke, B., R. Reuter, R. Heuermann, H. Wang, M. Babin and J. C. Therriault, 1997: Light absorption and fluorescence properties of chromophoric dissolved organic matter CDOM, in the St. Lawrence Estuary Case 2 waters. *Cont. Shelf Res.,* (17)3, 235–252.
Obernosterer, I., B. Reitner and G. J. Herndl, 1999: Contrasting effects of solar radiation on dissolved organic matter and its bioavailability to marine bacterioplankton. *Limn. Oceanogr.,* 447, 1645–1654.

Obernosterer, I., R. Sempere and G.J. Herndl, 2001: Ultraviolet radiation induces reversal of the bioavailability of DOM to marine bacterioplanton. *Aq. Microb. Ecol.,* 24(1), 61–68.
Ohlmann, J.C. and D.A. Siegel, 2000: Ocean radiant heating. Part II: Parameterizing solar radiation transmission through the upper ocean. *J. Phys Oceanogr.,* 30, 1849–1865.
Ohlmann, J.C., D.A. Siegel and C. Gautier, 1996: Ocean mixed layer radiant heating and solar penetration: A global analysis. J. *Climate.,* 9, 2265–2280.
Owens, T.G., A.P. Shreve and A.C. Albrecht, 1993: Dynamics and mechanism of singlet energy transfer between carotenoids and chlorophylls: light-harvesting and nonphotochemical fluorescence quenching. In: *Research in Photosynthesis* Vol. IV., N. Murata, Kluwer Academic Publishers, Dordrecht, 179–186.
Paulson, C.A. and J.J. Simpson, 1977: Irradiance measurements in the upper ocean. *J. Phys. Oceanogr., 7*, 953–956.
Plueddemann, A.J. and R.A. Weller, 1999: Structure and evolution of the oceanic surface boundary layer during the Surface Waves Processes Program. *J. Mar. Sys.*, 21, 85–102.
Prasil, O., N. Adir and I. Ohad, 1992: Dynamics of Photosystem II: mechanism of photoinhibition and recovery processes. In: *The Photosystem: Structure, Function and Molecular Biology.* J. Barber, Elsevier Publishers, Amsterdam, 295–348.
Preisendorfer, R.W., 1976: *Hydological Optics*. U.S. Dept. of Commerce, NOAA, Honolulu.
Preiswerk, D. and R.G. Najjar, 2000: A global, open-ocean model of carbonyl sulfide and its air-sea flux. *Global Biogeochemical Cycles,* 14(2), 585–598.
Price, J.F., R.A. Weller and R. Pinkel, 1986: Diurnal cycling: Observations and models of the upper ocean response to diurnal heating, cooling, and wind mixing. *J. Geophys. Res.,* 91C7, 8411–8427.
Riley, G.A., 1946: Factors controlling phytoplankton populations on Georges Bank. *Jour. Mar. Res.,* 6, 114–125.
Rochell-Newall, E.J., T.R. Fisher, C. Fan and P.M. Gilbert, 1999: Dynamics of chromophoric dissolved organic matter and dissolved organic carbon in experimental mesocosms. *Helgoland Marine Research,* 55(1), 12–22.
Salonen, K. and A. Vähätalo, 1994: Photochemical mineralisation of dissolved organic matter in Lake Skjervatjern. *Environ Int.,* 20, 307–312.
Sathyendranath, S., A.D. Gouveia, S.R. Shetye, P. Ravindran and T. Platt, 1991: Biological control of surface temperature in the Arabian Sea. *Nature,* 34(9), 54–56.
Schofield, O., T. Bergmann, W.P. Bissett, F. Grassle, D. Haidvogel, J. Kohut, M. Moline and S. Glenn, 2001: Linking regional coastal observatories to provide the foundation for a national ocean observation network. *Journal of Oceanic Engineering, in press.*
Schofield, O., J. Grzymski, W.P. Bissett, G.J. Kirkpatrick, D.F. Millie, M. Moline and C.S. Roesler, 1999: Optical monitoring and forecasting systems for harmful algal blooms, Possibility or pipe dream? *Journal of Phycology,* 35(6), 1477-1496.
Schofield, O., J. Grzymski, M.A. Moline and R.V.M. Jovine, 1998: Impact of temperature on photosynthesis in the red-tide dinoflagellate *Alexandrium fundyense Ca28. J. Plank. Res.,* 20, 1241–1258.
Schofield, O., B.B. Prezelin and G. Johnsen, 1996: Wavelength dependency in the photosynthetic parameters for two dinoflagellate species *Heterocapsa pygmaea* and *Prorocentrum minimum,* implications for the bio-optical modeling of photosynthetic rates. *J. Phycol.,* 32, 574–583.
Schofield, O., B.B. Prezelin and B.M.A. Kroon, 1995: Impact of ultraviolet-B radiation on photosystem II activity and its relationship to the inhibition of carbon fixation rates for Antarctic ice algae communities. *J. Phycol.,* 31, 703–715.
Schopf, J., 1993: Microfossils of the early Archean Apex Chart, new evidence of the antiquity of life. *Science,* 260, 640–646.
SCOR, 1990: *The Joint Global Ocean Flux Study.* International Council of Scientific Unions, Halifax.
Siegel, D.A. and A.F. Michaels, 1996: Quantification of non-algal light attenuation in the Sargasso Sea, Implications for biogeochemistry and remote sensing. *Deep Sea Res. II,* 43(2-3), 321–345.
Siegel, D.A., J.C. Ohlmann, L. Washburn, R.R. Bidigare, C.T. Nosse, E. Fields and Y. Zhou, 1995: Solar radiation, phytoplankton pigments and the radiant heating of the equatorial Pacific warm pool. *J. Geophys. Res.,* 100C3, 4885–4891.
Sivalingham, P.M., T. Ikawa and K. Nisizawa, 1974: Possible physiological roles of a substance showing characteristic UV-absorbing patterns in some marine phytoplankton. *Plant Cell Physiol.,* 15, 583–586.
Smith, C.M. and R.S. Alberte, 1994: Characterization of *in vivo* absorption features of chlorophyte, phaeophyte, and rhodophyte algal species. *Mar. Biol.,* 118, 511–521.
Taylor, A.H., A.J. Watson, M. Ainsworth, J.E. Robertson and D.R. Turner, 1991: A modelling investigation of the role of phytoplankton in the balance of carbon at the surface of the North Atlantic. *Global Biogeochemical Cycles,* 5(2), 151–171.
Telfer, A. and J. Barber, 1994. Elucidating the molecular mechanisms of photoinhibition by studying isolated photosystem II reaction centers. Photoinhibition of Photosynthesis from Molecular mechanisms to the Field. N.R. a. J.R.B. Baker. Oxford, *BIOS Scientific Publ.,* 25–45.
Tsujino, I., K. Yabe and I. Sekekawa, 1980: Isolation and structure of a new amino acid, shinorine, from the red alga *Chondrus yendoi. Bot. Mar.,* 23, 63–68.
Uher, G. and M.O. Andrea, 1997: Photochemical production of carbonyl sulfide in North Sea water, a process study. *Limn. Oceanogr.,* 42(3), 432–442.
Vähätalo, A.V., M. Salkinoja-Salonen, P. Taalas and K. Salonen, 2000: Spectrum of quantum yield for photochemical mineralization of dissolved organic carbon in a humic lake. *Limn. Oceanogr.,* 45, 664–676.
Valentine, R.L. and R.G. Zepp, 1993: Formation of carbon monoxide from the photodegradation of terrestrial dissolved organic carbon in natural waters. *Environ. Sci. Tech.,* 27, 409–412.
Vernet, M. and K. Whitehead, 1996: Release of ultraviolet-absorbing compounds by the red-tide dinoflagellate *Lingulodinium polyedra. Marine Biology*, 127, 35–44.
Vincent, W.F. and S. Roy, 1993: Solar ultraviolet-B radiation and aquatic primary production, damage, protection and recovery. *Environ. Rev.,* 1, 1–12.
Vodacek, A., N.V. Blough, M.D. DeGrandpre, E.T. Peltzer and R.K. Nelson, 1997. Seasonal variation of CDOM and DOC in the Middle Atlantic Bight, terrestrial inputs and photooxidation. *Limn. Oceanogr.,* 42(4), 674–686.
Walsh, J.J., 1975: A spatial simulation model of the Peru upwelling ecosystem. *Deep-Sea Res.,* 22, 201–236.
Walsh, J.J., D.A. Dieterle, M.B. Meyers and F.E. Müller-Karger, 1989: Nitrogen exchange at the continental margin, a numerical study of the Gulf of Mexico. *Progress in Oceanography,* 23, 245–301.
Weiss, P.S., S.S. Andrews, J.E. Johnson and O.C. Zafiriou, 1995: Photoproduction of carbonyl sulfide in South Pacific Ocean waters as a function of irradiation wavelength. *Geophysical Research Letters,* 22, 215–218.
Wroblewski, J.S., J.L. Sarmiento and G.R. Flierl, 1988: An ocean basin scale model of plankton dynamics in the North Atlantic. *Global Biogeochemical Cycles,* 2(3), 199–218.
Xie, H., R.M. Moore and W.L. Miller, 1998: Photochemical production of carbon disulfide in seawater. *J. Geophys. Res.,* 103, 5331–5344.
Yentsch, C.S., 1957: A non-extractive method for the quantitative estimation of chlorophyll in algal cultures. *Nature,* 179, 1302–1304.
Yentsch, C.S., 1960: The influence of phytoplankton pigments on the colour of sea water. *Deep-Sea Res., 7*, 1–9.
Yentsch, C.S. and D.A. Phinney, 1989: A bridge between ocean optics and microbial ecology. *Limn. Oceanogr.,* 34(8), 1694–1705.
Zafiriou, O., 1977: Marine organic photochemistry previewed. *Marine Chemistry,* 5, 497–522.
Zepp, R.G., T.V. Callaghan and D.J. Erickson, 1995: Effects of increased solar ultraviolet radiation on biogeochemical cycles. *Ambio,* 24, 181–187.